

# Learning Deep Kernels for Non-Parametric Independence Testing

Nathaniel Xu *University of British Columbia*

XUNATHAN@CS.UBC.CA

Feng Liu *University of Melbourne*

FENG.LIU1@UNIMELB.EDU.AU

Danica J. Sutherland *University of British Columbia; Alberta Machine Intelligence Institute*

DSUTH@CS.UBC.CA

## Abstract

The Hilbert-Schmidt Independence Criterion (HSIC) is a powerful tool for nonparametric detection of dependence between random variables. It crucially depends, however, on the selection of reasonable kernels; commonly-used choices like the Gaussian kernel, or the kernel that yields the distance covariance, are sufficient only for amply sized samples from data distributions with relatively simple forms of dependence. We propose a scheme for selecting the kernels used in an HSIC-based independence test, based on maximizing an estimate of the asymptotic test power. We prove that maximizing this estimate indeed approximately maximizes the true power of the test, and demonstrate that our learned kernels can identify forms of structured dependence between random variables in various experiments.

## 1. Introduction

Independence testing, the question of using paired samples to determine whether a random variable  $X$  and another  $Y$  are associated with one another or if they are statistically independent, is one of the most common tasks across scientific and data-based fields. Traditional methods make strong parametric assumptions, for instance assuming that  $X$  and  $Y$  are jointly normal so that dependence is characterized by covariance, and/or operate only in limited settings, for instance the tabular setting of the celebrated  $\chi^2$  test or Fisher’s exact test. More recent widely-applicable tests have been developed for discrete distributions based on the  $\ell_1$  distance (Biau and Györfi, 2005) or multinomial log-likelihood (Györfi and Vajda, 2002). Using these methods on continuous data, however, requires a “bucketing” process, which does not work well for high-dimensional data.

As an alternative for more general kinds of data distributions, Gretton et al. (2005) introduced the Hilbert-Schmidt Independence Criterion (HSIC), which measures the total cross-covariance between feature functions of  $X$  and  $Y$ , supporting even *infinite-dimensional* features in a reproducing kernel Hilbert space (RKHS). This statistic can also be efficiently estimated from samples. With appropriate choices of kernel (see Szabó and Sriperumbudur, 2018), HSIC tests can eventually detect *any* form of dependence between random variables, given enough samples. In a separate line of work, Székely et al. (2007) and Lyons (2013) proposed *distance covariance* tests, which measure the covariance of pairwise distances between  $X$  values with distances between  $Y$  values; it was later shown that these classes of tests are in fact equivalent (Sejdinovic et al., 2013).

With standard kernels, such as the Gaussian kernel or the distance kernel that recovers distance covariance, these tests will *eventually* be able to detect any fixed dependence with enough samples; indeed, most applications of HSIC or the distance covariance use these “default” choices. Their finite-sample behavior, however, can differ dramatically based on the choice of kernel. Dependence which is easy to identify with the “right lens” might be extremely subtle with another choice of how to “look at” the data, and require an enormous number of samples to achieve acceptable power.

Figure 1 shows the test power of HSIC with a simple kernel on a high-dimensional Gaussian mixture dataset. Choosing the lengthscales of a Gaussian kernel with the common median heuristic (HSIC-M) works reasonably in dimension 4, but requires enormous amounts of data in dimension 20 or 40. Optimizing the lengthscales for test power – HSIC-O with our scheme, or the previous approach HSIC-Agg (Schrab et al., 2023) – does not substantially help, because

arXiv:2409.06890v1 [stat.ML] 10 Sep 2024

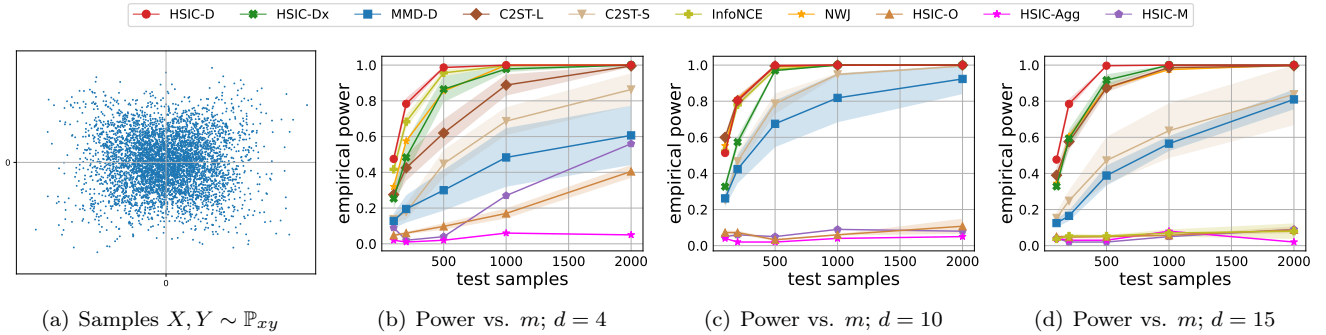


Figure 1: Vanilla kernel-based HSIC tests struggle on high-dimensional data. (a) A bimodal Gaussian mixture, with visible dependence between  $X$  and  $Y$ . (b)-(d) Test power as we add an increasing number of independent noise dimensions. When  $d = 4$  the median heuristic (HSIC-M) confidently detects dependence between  $X$  and  $Y$  with a reasonably large sample size, but struggles when  $d = 10$  or  $d = 15$ . Our method (HSIC-D) detects dependence in high dimensions with many fewer samples.

any Gaussian kernel is poorly suited to this task. Our scheme, however, allows optimizing the parameters of kernels defined by a deep network (HSIC-D), identifying a good kernel and achieving high test power with far fewer samples. Using a rich class of kernels parameterized by a deep neural network allows us to effectively identify dependence even between complex data types. With appropriate deep kernel architectures, we can maintain the consistency of the test, while achieving far more powerful tests at a given dataset size.

Our criterion for which kernel to select is based on the test power, whose asymptotic expression is dominated by the ratio of the HSIC to its standard deviation. We show that we can estimate this quantity from finite samples in a reliable way, such that optimizing the estimate approximately optimizes the asymptotic power of the test. To the best of our knowledge, this is the first theoretical analysis of general kernel selection in independence testing. We then construct a valid test via data splitting and permutation testing (e.g. Rindt et al., 2021). Our overall scheme builds on prior work in kernel two-sample testing (Gretton, Sriperumbudur, et al., 2012; Jitkrittum et al., 2016; Sutherland et al., 2017; Liu et al., 2020), but the important independence testing setting has thus far been unaddressed to our knowledge. We also demonstrate the effectiveness of our scheme in numerical experiments.

## 2. Kernel Independence Testing

**Problem 1** (Independence testing). *Let  $Z = (X, Y) \sim \mathbb{P}_{xy}$  on a domain  $\mathcal{X} \times \mathcal{Y}$ , and  $\mathbb{P}_x$  and  $\mathbb{P}_y$  the corresponding marginal distributions on  $\mathcal{X}$  and  $\mathcal{Y}$ . We observe  $m$  independent samples  $\{(x_1, y_1), \dots, (x_m, y_m)\}$  from  $\mathbb{P}_{xy}$ . We conduct a null hypothesis significance test, with the null hypothesis  $\mathfrak{H}_0 : \mathbb{P}_{xy} = \mathbb{P}_x \times \mathbb{P}_y$  (so  $X \perp Y$ ), and the alternative  $\mathfrak{H}_1 : \mathbb{P}_{xy} \neq \mathbb{P}_x \times \mathbb{P}_y$  (i.e.  $X \not\perp Y$ ).*

We wish to solve this problem without making strong (parametric) assumptions about the form of  $\mathbb{P}_{xy}$ ,  $\mathbb{P}_x$ , or  $\mathbb{P}_y$ . Most independence tests are based on estimating the “amount” of dependence between  $X$  and  $Y$ , or equivalently the discrepancy between  $\mathbb{P}_{xy}$  and  $\mathbb{P}_x \times \mathbb{P}_y$ . Given a nonnegative quantity which is zero if  $X \perp Y$ , we can reject  $\mathfrak{H}_0$  if our estimate is large enough that we are confident the true value is positive.

One well-known such measurement of dependence is the (Shannon) mutual information. This quantity, the Kullback-Liebler divergence of  $\mathbb{P}_{xy}$  from  $\mathbb{P}_x \times \mathbb{P}_y$ , is zero if and only if  $X \perp Y$ . Unfortunately, despite substantial work on estimating the mutual information in ways based on binning, nearest-neighbors, kernel density estimation, and so on (see e.g. the broad list implemented by Szabó 2014) or an array of approaches based on variational bounds estimated

with deep networks (e.g. Poole et al., 2019), the mutual information is fundamentally extremely difficult to estimate from samples (Paninski, 2003; McAllester and Stratos, 2020; J. Song and Ermon, 2020).

The Hilbert-Schmidt Independence Criterion (HSIC, Gretton et al., 2005), is also zero if and only if  $X$  and  $Y$  are independent when an appropriate kernel is chosen. Unlike the mutual information, it is easy to estimate from samples. We will discuss its relationship to mutual information in Section 3.

**Hilbert-Schmidt Independence Criterion (HSIC).** To define HSIC, we will first briefly review positive-definite kernels. A (real-valued) *kernel* is a function  $k : \mathcal{X} \times \mathcal{X} \rightarrow \mathbb{R}$  which can be expressed as the inner product between *feature maps*  $\phi : \mathcal{X} \rightarrow \mathcal{F}$ ,  $k(x, x') = \langle \phi(x), \phi(x') \rangle_{\mathcal{F}}$ , where  $\mathcal{F}$  is any Hilbert space. For every kernel function, there exists a unique space called the *reproducing kernel Hilbert space* (RKHS), which consists of functions  $f : \mathcal{X} \rightarrow \mathbb{R}$ . The key *reproducing property* of an RKHS  $\mathcal{F}$  states that for any function  $f \in \mathcal{F}$  and any point  $x \in \mathcal{X}$ , we have  $\langle f, \phi(x) \rangle_{\mathcal{F}} = f(x)$ .

Suppose we have a kernel  $k$  on  $\mathcal{X}$  with RKHS  $\mathcal{F}$  and feature map  $\phi$ , as well as another kernel  $l$  on  $\mathcal{Y}$  with RKHS  $\mathcal{G}$  and feature map  $\psi$ . Let  $\otimes$  denote the outer product.<sup>1</sup> The *cross-covariance operator* is

$$C_{xy} = \mathbb{E}_{xy} \left[ (\phi(x) - \mathbb{E}_x \phi(x)) \otimes (\psi(y) - \mathbb{E}_y \psi(y)) \right];$$

for kernels with finite-dimensional feature maps, this is exactly the standard (cross-)covariance matrix between the features of  $X$  and those of  $Y$ . Under mild integrability conditions on the kernel and the distributions,<sup>2</sup> the reproducing property shows that  $\langle f, C_{xy}g \rangle = \text{Cov}(f(X), g(Y))$  for all  $f \in \mathcal{F}$ ,  $g \in \mathcal{G}$ . One definition of independence is whether there exist any correlated “test functions”  $f$  and  $g$ . Thus, for rich enough choices of kernel – using universal  $k$  and  $l$  suffices, but is not necessary (Szabó and Sriperumbudur, 2018) – we have that  $X \perp\!\!\!\perp Y$  if and only if the operator  $C_{xy} = 0$ . We can thus check whether the operator is zero, and hence whether  $X \perp\!\!\!\perp Y$ , by checking the squared Hilbert-Schmidt norm of  $C_{xy}$ ,  $\text{HSIC}(X, Y) = \|C_{xy}\|_{\text{HS}}^2$ . With finite-dimensional features, this corresponds to the squared Frobenius norm of the feature cross-covariance matrix.

There are two similar estimators of HSIC in wide use. One, “the biased estimator,” is a  $V$ -statistic:

$$\widehat{\text{HSIC}}_{\text{b}}(X, Y) = \frac{1}{m^2} \text{tr}(\mathbf{KHLH}) = \frac{1}{m^2} \sum_{i,j} k_{ij}l_{ij} + \frac{1}{m^4} \sum_{i,j,q,r} k_{ij}l_{qr} - \frac{2}{m^3} \sum_{i,j,q} k_{ij}l_{iq}, \quad (1)$$

where here  $\mathbf{K}$  is the  $m \times m$  matrix with entries  $k_{ij} = k(x_i, x_j)$ ,  $\mathbf{L}$  similarly has entries  $l_{ij} = l(y_i, y_j)$ , and  $\mathbf{H}$  is the “centering matrix”  $\mathbf{I}_m - \frac{1}{m} \mathbf{1}_m \mathbf{1}_m^{\top}$ . This estimator has  $\mathcal{O}(1/m)$  bias, but is consistent.

The other common estimator, “the unbiased estimator,” is a  $U$ -statistic (L. Song et al., 2012):

$$\widehat{\text{HSIC}}_{\text{u}}(X, Y) = \frac{1}{m(m-3)} \left[ \text{tr}(\tilde{\mathbf{K}}\tilde{\mathbf{L}}) + \frac{\mathbf{1}^{\top} \tilde{\mathbf{K}} \mathbf{1} \mathbf{1}^{\top} \tilde{\mathbf{L}} \mathbf{1}}{(m-1)(m-2)} - \frac{2 \mathbf{1}^{\top} \tilde{\mathbf{K}} \tilde{\mathbf{L}} \mathbf{1}}{m-2} \right], \quad (2)$$

where  $\tilde{\mathbf{K}}$  and  $\tilde{\mathbf{L}}$  are  $m \times m$  matrices whose diagonal entries are zero but whose off-diagonal entries agree with those of  $\mathbf{K}$  or  $\mathbf{L}$ . It is unbiased,  $\mathbb{E} \widehat{\text{HSIC}}_{\text{u}}(X, Y) = \text{HSIC}(X, Y)$ , and also consistent.

**HSIC tests.** To construct a test, we use the asymptotic distribution of the unbiased HSIC estimator.

**Proposition 2** (L. Song et al., 2012, Theorem 5). *Under the alternative hypothesis  $\mathfrak{H}_1 : \mathbb{P}_{xy} \neq \mathbb{P}_x \times \mathbb{P}_y$ , the unbiased estimator of HSIC is asymptotically normal: with  $m$  samples,*

$$\sqrt{m}(\widehat{\text{HSIC}}_{\text{u}} - \text{HSIC}) \xrightarrow{d} \mathcal{N}(0, \sigma_{\mathfrak{H}_1}^2). \quad (3)$$

1. Analogously to Euclidean outer products,  $f \otimes g : \mathcal{G} \rightarrow \mathcal{F}$  is given by  $[f \otimes g]g' = f \langle g, g' \rangle_{\mathcal{G}}$ .

2. We require  $\mathbb{E}[\sqrt{k(x, x)}], \mathbb{E}[\sqrt{k(y, y)}] < \infty$ ; this is guaranteed for any distribution when  $k$  is bounded.

The asymptotic variance of  $\sqrt{m}\widehat{\text{HSIC}}_u$ ,  $\sigma_{\mathfrak{H}_1}^2$ , can be consistently estimated from  $n$  samples<sup>3</sup> as  $16(R - \text{HSIC}^2)$ , where  $R = \frac{1}{n} \sum_{i=1}^n \left( \frac{(n-4)!}{(n-1)!} \sum_{(j,q,r) \in \mathfrak{i}_3^n / \{i\}} h(i, j, q, r) \right)^2$ . Here  $\mathfrak{i}_n^\ell \setminus \{i\}$  denotes the set of all  $\ell$ -tuples drawn without replacement from the set  $\{1, \dots, n\} \setminus \{i\}$ , and  $h(i, j, q, r) = \frac{1}{24} \sum_{(s,t,u,v) \in \binom{\{i,j,q,r\}}{4}} k_{st}(l_{st} + l_{uv} - 2l_{su})$ , where the sum ranges over all  $4! = 24$  ways to assign the distinct indices  $\{i, j, q, r\}$  to the four variables  $(s, t, u, v)$  without replacement.

The behavior of the estimator is different under the null,  $X \perp\!\!\!\perp Y$ ; then  $m\widehat{\text{HSIC}}_u$  (rather than  $\sqrt{m}\widehat{\text{HSIC}}_u$ ) converges in distribution to something with complex dependence on  $\mathbb{P}_x, \mathbb{P}_y, k$ , and  $l$ .

Thus, under  $\mathfrak{H}_0$  when  $\text{HSIC} = 0$ , the statistic  $m\widehat{\text{HSIC}}_u$  has mean zero and standard deviation  $\Theta(1)$ . Under  $\mathfrak{H}_1$ , the mean of  $m\widehat{\text{HSIC}}_u = \Theta(\sqrt{m}) \rightarrow \infty$ , with standard deviation  $\Theta(\sqrt{m})$ . For large enough  $m$ , these two cases are distinguishable. To select a threshold at any particular  $m$ , we use permutation testing to estimate the  $1 - \alpha$  quantile of the null distribution: we repeatedly randomly shuffle the data to break any possible dependence between  $X$  and  $Y$ , and estimate the  $1 - \alpha$  quantile of the distribution of  $m\widehat{\text{HSIC}}_u$  values computed on shuffled samples. If we also include the original order of the data in the shuffled set, this scheme is exactly valid for any number of permutations (Hemerik and Goeman, 2018, Theorem 2), and yields a consistent test (Rindt et al., 2021).

**Impact of kernel selection.** Two-sample testing (given samples from  $\mathbb{P}$  and  $\mathbb{Q}$ , is  $\mathbb{P} = \mathbb{Q}$ ?) is closely related to independence testing, where kernel-based methods similar to HSIC are in wide use. Similarly to independence testing, any “reasonable” choice of kernel gives a consistent test, such that a casual user might think they can simply always use a Gaussian kernel with unit bandwidth and be done with it. In practice, however, this scheme can perform extremely poorly; if the data varies on a very different scale, it will take exorbitant quantities of data to achieve any reasonable test power. Thus, users of Gaussian kernels in two-sample testing often use the *median heuristic* to choose a kernel relevant to the data at hand, choosing a bandwidth based on the median pairwise distance among data points (Gretton, Borgwardt, et al., 2012). While this is a reasonable first guess for many data types, there exist datasets where it can be dramatically better to instead select a bandwidth that optimizes a measure of test power (Gretton, Sriperumbudur, et al., 2012; Sutherland et al., 2017). Beyond that, there exist many distributions where no Gaussian kernel performs well – for instance, many problems on natural image data or involving sparsity – but a learned deep kernel can yield very powerful tests (Liu et al., 2020).

Although it has not been to our knowledge studied in the same way, the situation is analogous for independence testing. The synthetic HDGM dataset (for “high-dimensional Gaussian mixture”; details in Section 6) is a mixture of two Gaussians, where two dimensions are dependent (but uncorrelated), while all other dimensions are independent of one another. Splitting this  $Z$  into  $X$  and  $Y$  such that one of the dependent dimensions is in each variable, detecting this dependence becomes quite difficult when there are many “distractor” dimensions present.

Several independence tests are considered in Figure 1, including HSIC-M based on a median-heuristic Gaussian kernel, HSIC-O based on optimizing the lengthscale of a Gaussian with our scheme (introduced shortly), and HSIC-D which uses our scheme to learn a kernel parameterized by a deep network. (Others are described in Section 6). Kernel selection significantly influences the test power. Optimizing the lengthscale of the Gaussian helps a bit, but much more improvement comes from using a more complex deep kernel class – an option made available by our optimization scheme.

### 3. Relationship to Mutual Information Bounds

**Population values.** Mutual information,  $I(X; Y)$ , is also frequently used to measure the dependence among two random variables. As mentioned, estimation is fundamentally challenging. Recent approaches focus on finding variational bounds on  $I(X; Y)$  which can themselves be easily estimated. As an example, consider the following lower bound (van den Oord et al., 2018; Poole et al., 2019), named for its connection to noise-contrastive estimation

3. Typically  $m = n$ , but we might want to use a few ( $n$ ) samples to roughly estimate the power of an  $m$ -sample test with  $m \gg n$ , as done in a different context by Sutherland and Deka (2019) and Deka and Sutherland (2023).

(Gutmann and Hyvärinen, 2012):

$$I_{\text{NCE}}^{f,K}(X; Y) = \mathbb{E}_{(x_i, y_i) \sim \mathbb{P}_{xy}^K} \left[ \hat{I}_{\text{NCE}}^{f,K} \right] \leq I(X; Y) \quad \hat{I}_{\text{NCE}}^{f,K} = \frac{1}{K} \sum_{i=1}^K \log \frac{e^{f(x_i, y_i)}}{\frac{1}{K} \sum_{j=1}^K e^{f(x_i, y_j)}}.$$

Typically we parameterize  $f$  as a deep network, and estimate  $I_{\text{NCE}}^{f,K}$  from samples with  $\hat{I}_{\text{NCE}}^{f,K}$ . To choose  $f$ , we maximize  $\hat{I}_{\text{NCE}}^{f,K}$  on minibatches, attempting to find the tightest lower bound.

To understand the relationship to HSIC, we first use the equivalence to the maximum mean discrepancy (MMD), a notion of distance between distributions, in its integral probability metric form.

**Proposition 3** (Gretton, Borgwardt, et al., 2012, Theorem 25). *Let  $k$  and  $l$  be kernels on  $\mathcal{X}$  and  $\mathcal{Y}$ , and define a kernel on  $\mathcal{X} \times \mathcal{Y}$  by  $h((x, y), (x', y')) = k(x, x')l(y, y')$  with RKHS  $\mathcal{H}$ . Then*

$$\sqrt{\text{HSIC}(X, Y)} = \text{MMD}(\mathbb{P}_{xy}, \mathbb{P}_x \times \mathbb{P}_y) = \sup_{\substack{f \in \mathcal{H} \\ \|f\|_{\mathcal{H}} \leq 1}} \mathbb{E}_{(X, Y) \sim \mathbb{P}_{xy}} [f(X, Y)] - \mathbb{E}_{\substack{X \sim \mathbb{P}_x \\ Y' \sim \mathbb{P}_y}} [f(X, Y')].$$

Now suppose  $\sup_{x \in \mathcal{X}, y \in \mathcal{Y}} h((x, y), (x, y)) \leq \nu^2$  for  $\nu \geq 0$ . Then  $|f(x, y)| = |\langle f, \phi_h(x, y) \rangle_{\mathcal{H}}| \leq \nu \|f\|_{\mathcal{H}}$  by Cauchy-Schwarz, and so  $\|f\|_{\mathcal{H}} \geq \frac{1}{\nu} \sup_{x, y} |f(x, y)| = \frac{1}{\nu} \|f\|_{\infty}$ . We thus have that

$$\sqrt{\text{HSIC}(X, Y)} \leq \sup_{f: \|f\|_{\infty} \leq \nu} \mathbb{E}_{(X, Y) \sim \mathbb{P}_{xy}} [f(X, Y)] - \mathbb{E}_{\substack{X \sim \mathbb{P}_x \\ Y' \sim \mathbb{P}_y}} [f(X, Y')] = 2\nu \text{TV}(\mathbb{P}_{xy}, \mathbb{P}_x \times \mathbb{P}_y), \quad (4)$$

where TV is the total variation distance between distributions (Sriperumbudur et al., 2012)<sup>4</sup> Applying standard bounds relating the total variation to the KL divergence which defines mutual information, we obtain the following.

**Proposition 4.** *In the setting of Proposition 3, suppose  $\sup_{x \in \mathcal{X}, y \in \mathcal{Y}} h((x, y), (x, y)) \leq \nu^2$ . Then*

$$\frac{1}{2\nu^2} \text{HSIC}(X, Y) \leq I(X; Y) \quad \text{and} \quad -\log \left( 1 - \frac{1}{4\nu^2} \text{HSIC}(X, Y) \right) \leq I(X; Y).$$

*Proof.* The first bound follows from applying Pinsker’s inequality, which relates total variation to the KL divergence, to (4). The second instead applies the bound of Bretagnolle and Huber (1978) (also see Canonne, 2023).  $\square$

The second bound is tighter for large values of  $I(X; Y)$ ; most importantly, both bounds are monotonic in  $\text{HSIC}(X, Y)/\nu^2$ .

We could thus consider a similar scheme to prior work: choose kernels  $k, l$  to maximize a mutual information lower bound, by maximizing  $\text{HSIC}(X, Y)/\nu^2$ . Indeed, maximizing HSIC has been used by many previous applications in other areas (e.g. Blaschko and Gretton, 2009; L. Song et al., 2012; Y. Li et al., 2021; Dong et al., 2023).

**Tests.** To construct an appropriate test and avoid overfitting, we choose a kernel on a training set, then run a test on a separate test set.

We can also use the same scheme to construct an independence test based on  $I_{\text{NCE}}$ , which to our knowledge has not yet been done in the literature. Given a critic function  $f$  chosen independently of a test dataset – perhaps obtained by maximizing  $\hat{I}_{\text{NCE}}$  on a training set, but not necessarily – we can again construct a permutation test with exact level control based on the test statistic

$$\hat{I}_{\text{NCE}}^{f,K} = \frac{1}{K} \sum_{i=1}^K f(x_i, y_i) - \frac{1}{K} \sum_{i=1}^K \log \left( \frac{1}{K} \sum_{j=1}^K e^{f(x_i, y_j)} \right). \quad (5)$$

4. Sriperumbudur et al. (2012) define the TV as twice the more common definition, which we use here.

The second term of (5) considers all pairs  $x_i, y_j$ , regardless of how they are aligned in the dataset. Thus it shifts all permutations by the same amount, and is irrelevant to the actual test. The same is true for many mutual information bounds, including UBA, TUBA, NWJ, and DV considered by Poole et al. (2019); they choose  $f$  differently, but given an  $f$ , permutation tests are identical.

Now consider a test based on  $\text{MMD}(\mathbb{P}_{xy}, \mathbb{P}_x \times \mathbb{P}_y)$  using a kernel of the form  $h((x, y), (x', y')) = g(x, y)g(x', y')$  for some real-valued function  $g$ . (If  $g(x, y) = g_1(x)g_2(y)$ , this is an HSIC test.) Because  $\phi_h(x, y) = g(x, y) \in \mathbb{R}$  is a valid feature map, every function in  $\mathcal{H}$  is of the form  $f(x, y) = \alpha g(x, y)$  with  $\|\alpha g\|_{\mathcal{H}} = |\alpha|$ . By Proposition 3,

$$\text{MMD}(\mathbb{P}_{xy}, \mathbb{P}_x \times \mathbb{P}_y)^2 = \left( \sup_{|\alpha| \leq 1} \alpha (\mathbb{E} g(X, Y) - \mathbb{E} g(X, Y')) \right)^2 = (\mathbb{E} g(X, Y) - \mathbb{E} g(X, Y'))^2.$$

Using the plug-in estimator corresponding to the biased HSIC estimator (1) would yield the test statistic

$$\widehat{\text{HSIC}}_{\text{b}} = \left( \frac{1}{m} \sum_{i=1}^m g(x_i, y_i) - \frac{1}{m^2} \sum_{i=1}^m \sum_{j=1}^m g(x_i, y_j) \right)^2. \quad (6)$$

Comparing (6) to (5) with  $K = m$ , we can see that the main term is identical between the two; call this  $T$ . The other term is again permutation-invariant; it is the mean of  $T$  over all possible permutations,  $\bar{T}$ . Thus, a permutation test based on (6) asks how far the value of  $T$  for the true data is from  $\bar{T}$ , while a permutation test based on (5) is equivalent to asking how much the value of  $T$  exceeds  $\bar{T}$ . The only difference is that (6) gives a two-sided test, while (5) gives a one-sided test.<sup>5</sup>

Our usual test uses  $\widehat{\text{HSIC}}_{\text{u}}$  of (2) instead of  $\widehat{\text{HSIC}}_{\text{b}}$ , but the difference in estimators is typically small. Thus, if we use deep kernels of the form  $k(x, x') = f(x)f(x')$  and  $l(y, y') = g(y)g(y')$ , the HSIC test<sup>6</sup> is nearly equivalent to the NCE test with a separable critic function  $(x, y) \mapsto f(x)g(y)$ . The NCE test chooses a critic by maximizing the NCE estimate; while we could choose a (different) critic by maximizing the HSIC, we will now see there is a better approach.

## 4. Choosing an HSIC kernel

**Approximate test power.** The standard quality measure of a null hypothesis test, as long as it satisfies its design level of Type-I error, is *test power*: the probability that, when  $X \not\perp Y$ , we correctly reject  $\mathfrak{H}_0$ . Proposition 2 implies, using  $\Phi$  for the standard normal CDF, that

$$\begin{aligned} \Pr_{\mathfrak{H}_1} \left( m \widehat{\text{HSIC}}_{\text{u}} > r \right) &= \Pr_{\mathfrak{H}_1} \left( \frac{\sqrt{m}}{\sigma_{\mathfrak{H}_1}} (\widehat{\text{HSIC}}_{\text{u}} - \text{HSIC}) > \frac{r}{\sqrt{m} \sigma_{\mathfrak{H}_1}} - \frac{\sqrt{m} \text{HSIC}}{\sigma_{\mathfrak{H}_1}} \right) \\ &\sim \Phi \left( \frac{\sqrt{m} \text{HSIC}}{\sigma_{\mathfrak{H}_1}} - \frac{r}{\sqrt{m} \sigma_{\mathfrak{H}_1}} \right), \end{aligned} \quad (7)$$

where  $a \sim b$  means  $\lim_{m \rightarrow \infty} a/b = 1$ . Letting  $r$  be the threshold found by permutation testing, for any given  $\mathbb{P}_{xy}$ ,  $k$ , and  $l$ , we know from Proposition 2 that  $r$  converges to a constant and HSIC and  $\sigma_{\mathfrak{H}_1}$  are also constants. As  $m$  grows, the test power is thus dominated by the first term.<sup>7</sup> Thus, maximizing the following *approximate test power* maximizes the limiting power of the test as  $m \rightarrow \infty$ :

$$J(X, Y; k, l) = \frac{\text{HSIC}(X, Y; k, l)}{\sigma_{\mathfrak{H}_1}(X, Y; k, l)}. \quad (8)$$

5. Y. Li et al. (2021, Section 3.1) also found a relationship between HSIC and  $I_{\text{NCE}}$  for categorical  $Y$ .

6. This version is closely related to a witness two-sample test (Kübler et al., 2022) used for independence.

7. This statement, while true in the limit  $m \rightarrow \infty$ , does not fully describe the setting for smaller  $m$ : for instance, a test which is only near the rejection threshold will have  $r \approx m \text{HSIC}$ , in which case the two terms are of approximately equal size. As in Footnote 3, though, we can estimate the power of an  $m$ -sample test with  $n$  samples: here we use  $n$  samples to approximately maximize the power of a test with  $m \rightarrow \infty$  samples. Deka and Sutherland (2023) estimate an analogue of (7) rather than just (8) in a related setting.

In practice, we cannot evaluate  $J$  in (8), since we do not know  $\mathbb{P}_{xy}$ . Thus, we estimate  $J$  using

$$\hat{J}_\lambda(X, Y; k, l) = \frac{\widehat{\text{HSIC}}_{\mathfrak{u}}(X, Y; k, l)}{\hat{\sigma}_{\mathfrak{S}_1}^\lambda(X, Y; k, l)}, \quad (9)$$

using a regularized variance estimator  $\hat{\sigma}_{\mathfrak{S}_1}^\lambda(X, Y; k) = \sqrt{16(R - \widehat{\text{HSIC}}_{\mathfrak{u}}^2) + \lambda}$ . Here  $R$  is exactly the estimate from Proposition 2; following L. Song et al. (2012), it can be computed more efficiently with  $R = \frac{((n-4)!)^2}{4n((n-1)!)^2} \|\mathbf{h}\|^2$ , where the vector  $\mathbf{h}$  is

$$\begin{aligned} \mathbf{h} = & (n-2)^2 \left( \tilde{\mathbf{K}} \circ \tilde{\mathbf{L}} \right) \mathbf{1} - n(\tilde{\mathbf{K}}\mathbf{1}) \circ (\tilde{\mathbf{L}}\mathbf{1}) + (\mathbf{1}^\top \tilde{\mathbf{L}}\mathbf{1})\tilde{\mathbf{K}}\mathbf{1} + (\mathbf{1}^\top \tilde{\mathbf{K}}\mathbf{1})\tilde{\mathbf{L}}\mathbf{1} - (\mathbf{1}^\top \tilde{\mathbf{K}}\tilde{\mathbf{L}}\mathbf{1})\mathbf{1} \\ & + (n-2) \left( (\mathbf{1}^\top (\tilde{\mathbf{K}} \circ \tilde{\mathbf{L}})\mathbf{1})\mathbf{1} - \tilde{\mathbf{K}}\tilde{\mathbf{L}}\mathbf{1} - \tilde{\mathbf{L}}\tilde{\mathbf{K}}\mathbf{1} \right), \end{aligned}$$

with  $\circ$  denoting elementwise multiplication on matrices, and  $\mathbf{1} = (1, \dots, 1) \in \mathbb{R}^n$ . Given sets of possible kernels, we can approximately identify the kernels  $(k, l)$  yielding the asymptotically most powerful HSIC test by maximizing (9). Typically, we run some variant of a gradient-based optimization algorithm to maximize (9) with respect to the parameters of  $k$  and/or  $l$ .

**Kernel architecture.** Since simple kernels have limited power to observe the dependence between  $X$  and  $Y$ , we consider using deep kernels (Wilson et al., 2016), which have been successfully used in two-sample testing (Sutherland et al., 2017; Liu et al., 2020; Liu et al., 2021) and many other settings (e.g. C.-L. Li et al., 2017; Arbel et al., 2018; Jean et al., 2018; Y. Li et al., 2021).

Specifically, similarly to Liu et al. (2020), we use the following deep kernels for  $X$  and  $Y$ :

$$\begin{aligned} k_\omega(x, x') &= (1 - \epsilon_X) \kappa_X(f_\omega(x), f_\omega(x')) + \epsilon_X q_X(x, x') \\ l_\gamma(y, y') &= (1 - \epsilon_Y) \kappa_Y(g_\gamma(y), g_\gamma(y')) + \epsilon_Y q_Y(y, y'). \end{aligned}$$

Here  $f_\omega$  and  $g_\gamma$  are deep networks with parameters in  $\omega, \gamma$ , which extract relevant features from  $\mathcal{X}$  or  $\mathcal{Y}$  to a feature space  $\mathbb{R}^D$ . These features are then used inside a Gaussian kernel  $\kappa$  on the space  $\mathbb{R}^D$ , to compute the baseline “similarity” between data points. We then take a convex combination of that kernel with a Gaussian kernel  $q$  on the input space; the weight of this component is determined by a parameter  $\epsilon \in (0, 1)$ . Using  $\epsilon > 0$  provides a “backup” to the deep kernel, perhaps giving some signal early in optimization when the deep kernel features are not yet useful, and guaranteeing that the overall kernel is characteristic. The lengthscale of  $\kappa$  as well as the mixture parameter  $\epsilon$  are included in the overall parameters,  $\omega$  or  $\gamma$ , and learned during the optimization process.

With  $\epsilon = 0$ , scalar-output  $f_\omega$  and  $g_\gamma$ , and  $\kappa(a, b) = ab$ , we obtain the kernel used for the near-equivalence to mutual information-based tests in Section 3. Using non-scalar features and a more powerful  $\kappa$  allows the kernel to take on more of the “work,” and in most of the mentioned prior work has performed better than scalar features with linear  $\kappa$ .

**Overall learning algorithm.** The overall procedure, written based on full-batch gradient ascent for simplicity, is shown in Algorithm 1. In practice, we use AdamW (Loshchilov and Hutter, 2019) instead, and draw minibatches in epochs; experimental details are given in Appendix C.1.

Let  $E_X$  be the cost of computing an embedding  $f_\omega(x)$ ,  $E_Y$  be the cost of computing an embedding  $f_\gamma(y)$ , and  $L$  the cost of computing  $k_\omega(x, x')$  and  $l_\gamma(y, y')$  given the relevant embeddings. Each training iteration costs  $\mathcal{O}(KE_X + KE_Y + K^2L)$ , where  $K$  is the minibatch size. Typically for practical values of  $K$ ,  $E_X + E_Y \gg KL$ , so the cost is “almost” linear in practice.<sup>8</sup>

8. Equation (9) could use block estimators (Zaremba et al., 2014) or incomplete  $U$ -statistics (Blom, 1976) to reduce  $\mathcal{O}(K^2L)$  to  $\mathcal{O}(K^\beta L)$  for any  $\beta \leq 2$ , at the cost of increased variance (see Ramdas et al., 2015).

---

**Algorithm 1** Testing with a learned deep-HSIC

---

**Input:**  $S_Z = (S_X, S_Y)$ , various hyperparameters used below;  
 $\omega \leftarrow \omega_0; \gamma \leftarrow \gamma_0; \lambda \leftarrow 10^{-8}$ ; Split the data into  $S_Z^{\text{tr}} \cup S_Z^{\text{te}}; (S_X^{\text{tr}}, S_Y^{\text{tr}}) \leftarrow S_Z^{\text{tr}}; (S_X^{\text{te}}, S_Y^{\text{te}}) \leftarrow S_Z^{\text{te}};$   
*# Phase 1: train the kernel parameters  $\omega$  and  $\gamma$  on  $S_Z^{\text{tr}}$*   
**for**  $T = 1, 2, \dots, T_{\text{max}}$  **do**  
 $Z = (X, Y) \leftarrow \text{minibatch from } S_Z^{\text{tr}} = (S_X^{\text{tr}}, S_Y^{\text{tr}});$   
 $\hat{J}_\lambda(\omega, \gamma) \leftarrow \widehat{\text{HSIC}}_{\text{u}}(X, Y; k_\omega, l_\gamma) / \hat{\sigma}_{\hat{S}_1}^\lambda(X, Y; k_\omega, l_\gamma);$  *# as in Equation (9)*  
 $\omega \leftarrow \omega + \eta \nabla_\omega \hat{J}_\lambda(\omega, \gamma); \quad \gamma \leftarrow \gamma + \eta \nabla_\gamma \hat{J}_\lambda(\omega, \gamma);$  *# maximize  $\hat{J}_\lambda(\omega, \gamma)$*   
*# Phase 2: permutation test with  $k_\omega$  and  $l_\gamma$  on  $S_Z^{\text{te}}$*   
 $\text{perm}_0 \leftarrow \widehat{\text{HSIC}}_{\text{u}}(S_X^{\text{te}}, S_Y^{\text{te}}; k_\omega, l_\gamma)$  *# our main estimate*  
**for**  $i = 1, 2, \dots, n_{\text{perm}}$  **do**  
 $\text{perm}_i \leftarrow \widehat{\text{HSIC}}_{\text{u}}(\text{shuffle}(S_X^{\text{te}}), S_Y^{\text{te}}; k_\omega, l_\gamma)$  *# no need to shuffle both sets*  
**Output:**  $k_\omega, l_\gamma, \text{perm}_0, p\text{-value } \frac{1}{n_{\text{perm}}} \sum_{i=0}^{n_{\text{perm}}} \mathbb{1}(\text{perm}_i \geq \text{perm}_0)$

---

## 5. Theoretical Analysis

Does optimizing the estimator  $\hat{J}_\lambda$  of (9) in fact approximately optimize the asymptotic test power  $J$  in (8)? Theorem 5 shows that, if the training set size is reasonably large and we can optimize the estimates successfully, we can learn a kernel that generalizes nearly optimally and is hence powerful for large  $m$ , not just overfitting to the training set (and finding a bad test).

**Theorem 5.** *Under Assumptions (A) to (C), let  $\Theta \subseteq \Omega \times \Gamma$  be a set of kernel parameters  $\theta \in \Theta$  for which  $\sigma_\theta^2 \geq s^2$ , and  $n$  be the training set size; take  $\lambda = \Theta(n^{-1/3})$ . Then*

$$\sup_{\theta:=(\omega,\gamma)\in\Theta} \left| \hat{J}_\lambda(X, Y; k_\omega, l_\gamma) - J_\lambda(X, Y; k_\omega, l_\gamma) \right| = \tilde{\mathcal{O}}_p \left( \frac{1}{s^2 n^{1/3}} \left[ \frac{1}{s} + L_k + L_l + \sqrt{D_\Omega} + \sqrt{D_\Gamma} \right] \right).$$

If there are unique best kernels  $(k_{\omega^*}, l_{\gamma^*})$  maximizing  $J_\lambda(X, Y; k_\omega, l_\gamma)$ , then the maximizer of  $\hat{J}_\lambda(X, Y; k_\omega, l_\gamma)$  converges in probability to  $(k_{\omega^*}, l_{\gamma^*})$  as  $n \rightarrow \infty$ .

Appendix A states and proves a nonasymptotic version of this result; the assumptions and proof techniques are based on those of Liu et al. (2020).

## 6. Experiments

**Baselines.** We compare our method with various baselines, all based on permutation testing:

- HSIC-D: HSIC using deep kernels on each space  $\mathcal{X}$  and  $\mathcal{Y}$ ; simultaneously trained via Section 4.
- HSIC-Dx: HSIC using a tied deep kernel, i.e.  $k_\omega = l_\gamma$ , and trained via Section 4.
- HSIC-O: HSIC using Gaussian kernels, with each bandwidth parameter optimized via Section 4.
- HSIC-M: HSIC using Gaussian kernels, with bandwidth selected via the median heuristic.
- HSIC-Agg (Schrab et al., 2023): aggregating Gaussian kernels, with their default settings.
- MMD-D: The method of Liu et al. (2020) applied to  $\mathbb{P}_{xy}$  vs  $\mathbb{P}_x \times \mathbb{P}_y$ ,<sup>9</sup> with a kernel on  $\mathcal{X} \times \mathcal{Y}$ .
- C2ST-S (Lopez-Paz and Oquab, 2017) / C2ST-L (Cheng and Cloninger, 2022): Sign/logit-based classifier two-sample test for  $\mathbb{P}_{xy}$  vs  $\mathbb{P}_x \times \mathbb{P}_y$ .
- InfoNCE (van den Oord et al., 2018; Poole et al., 2019): the statistic  $\hat{I}_{\text{NCE}}$  as in Section 3.
- NWJ (Nguyen et al., 2010; Poole et al., 2019): another mutual information bound statistic  $\hat{I}_{\text{NWJ}}$ .

---

9. Specifically, we compare the given samples to a single shuffling of the given samples.



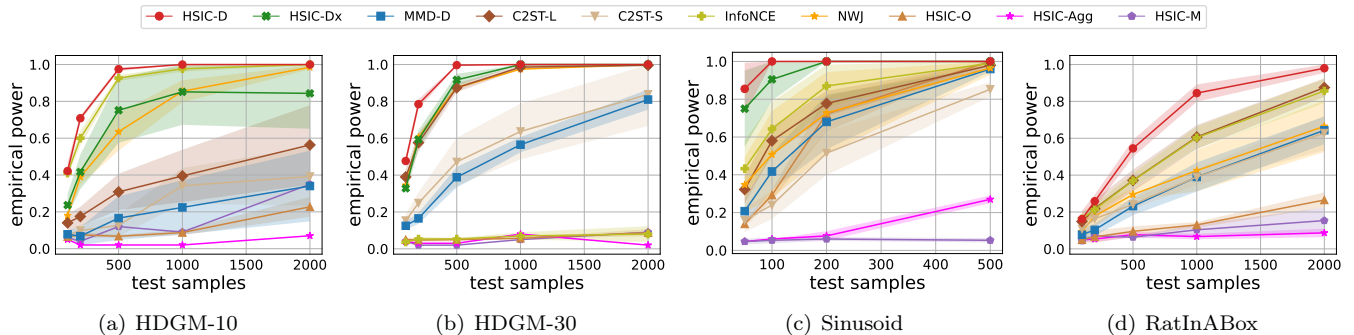


Figure 2: Empirical power vs sample size  $m$  for different datasets, when trained with a large training set. The average test power is computed over 5 training runs, where the empirical power is determined over 100 permutation tests. The shaded region covers one standard error from the mean.

**Datasets.** We consider three informative synthetic datasets, where the true answers are known.

- **High-dimensional Gaussian mixture.** The distribution HDGM- $d$  has  $d$  total dimensions (divided between  $X$  and  $Y$ ), but has dependence only between two of them:

$$[X_1, Y_{[d/2]}, \dots, X_{[d/2]}, Y_1] \sim \sum_{i=1}^2 \frac{1}{2} \mathcal{N} \left( \mathbf{0}_d, \begin{bmatrix} 1 & 0.5(-1)^i & \mathbf{0}_{d-2}^T \\ 0.5(-1)^i & 1 & \mathbf{0}_{d-2}^T \\ \mathbf{0}_{d-2} & \mathbf{0}_{d-2} & I_{d-2} \end{bmatrix} \right),$$

where the odd dimensions are taken to be from  $\mathbb{P}_x$  and even dimensions to be from  $\mathbb{P}_y$ . Moreover, for  $d \geq 4$  the dependent variables  $X_1$  and  $Y_{[d/2]}$  are at different dimensions. We perform independence tests at dimensions 4, 8, 10, 20, 30, 40, and 50.

- **Sinusoid** (Sejdinovic et al., 2012). We sample from sinusoidally dependent data with distribution  $\mathbb{P}_{xy} \propto 1 + \sin(\ell x) \sin(\ell y)$  on support  $\mathcal{X} \times \mathcal{Y} = [-\pi, \pi]^2$ . Higher frequencies  $\ell$  produce subtler departures from the uniform distribution, resulting in a harder independence problem; we use  $\ell = 4$ . A visualization of this density is given in Figure 9.

- **RatInABox** (George et al., 2024). RatInABox simulates hippocampal cells of a rat in motion. In particular, we test for dependence between firing rates of grid cells and the rat’s head direction. Grid cells respond near points in a grid covering the environment surface, and should be subtly connected to head direction because of the geometry of the “box” (Figure 8). We consider 8 grid cells, and simulate motion for 100 000 seconds, taking a measurement every 5 seconds as our dataset.

**Power versus test size.** We first compare how well methods identify dependency with a large available training set, by comparing the rate at which the learned tests achieve perfect power (1.0) as the test set size  $m$  increases. Results on the HDGM problems are given in Figures 1 and 5 for  $m$  in  $\{100, 200, 500, 1000, 2000\}$ . We use a training size of 10,000 for HDGM  $\leq 30$  and 100,000 for HDGM  $> 30$ , and 2000 validation samples for all dimensions. Overall, HSIC-D outperforms baselines, and is able to reach perfect power using smaller  $m$ . Both InfoNCE and C2ST-L also achieve high power at lower dimensions, but are unable to observe dependence for HDGM- $d$  with  $d \geq 40$ . Similarly, optimized bandwidth HSIC-O and median heuristic HSIC-M perform moderately well at lower dimensions, but at dimension of 15 and above fail to learn anything meaningful and exhibit power levels approximately equal to the type-I error rate.

Sinusoid results are shown in Figure 2 (d). We train on 5,000 samples and use 1,000 for validation. Once again, HSIC-D outperforms other baselines and can achieve perfect power using the smallest number of samples. In general, all methods apart from the median heuristic are able to detect dependency given enough test samples.

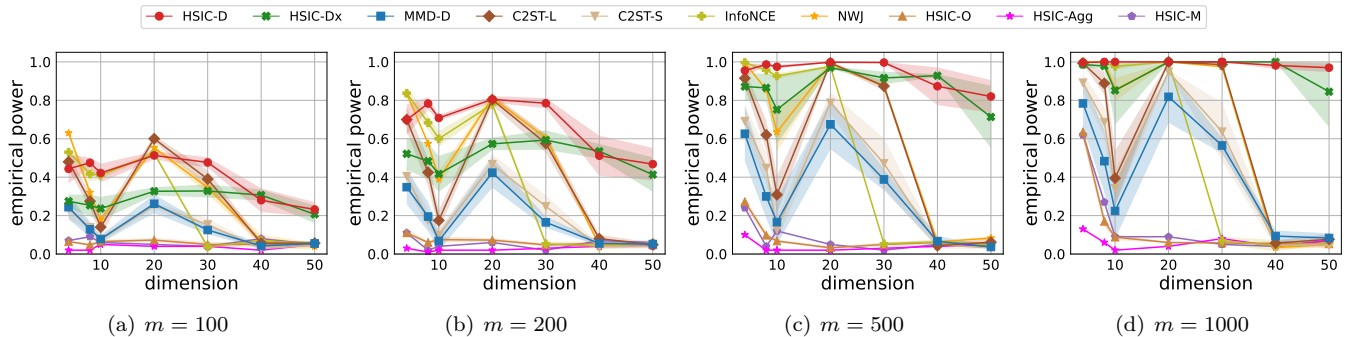


Figure 3: Empirical power vs dimension across various test sample sizes  $m = \{100, 200, 500, 1000\}$  for HDGM. The shaded region covers one standard error over 5 training runs.

RatInABox results are shown in Figure 2 (c). We use a training size of 4,000 samples with no validation. Again, HSIC-D exhibits higher empirical power than baselines. Notably, HSIC-Agg underperforms HSIC-O in these settings, despite considering a similar class of kernels. On these problems it seems that the aggregation process is worse than data splitting; more relevantly, data splitting and optimization allows for far more complex (deep) kernels than would be reasonable with a finite set of available kernels in HSIC-Agg.

**Power versus dimension.** We demonstrate the effectiveness of our method at various dimensions  $d/2$  by examining the empirical test power at HDGM- $d$  for  $d \in \{4, 8, 10, 20, 30, 40, 50\}$  with fixed test sizes  $m$ . We use the same training splits as before. Results are shown in Figure 3. HSIC-D still exhibits the highest test power across all dimensions. When a small number of test samples are used (i.e.,  $m = 100$ ) the performance of HSIC-D slightly degrades with increasing dimension, while at larger test sample sizes it consistently has near-perfect power. C2ST-L and InfoNCE demonstrate similar behavior but with worse power levels. HSIC-O and HSIC-M show failure at high dimensions. This is most noticeable at  $m = 2000$ , where the power levels drastically curve downwards with increasing dimension.

**Power versus dataset size.** A drawback to kernel selection via optimization is that we must hold out a split of the data for training. In contrast, HSIC-M and HSIC-Agg are able to utilize the entirety of the dataset for their test. To examine this trade-off, we consider consistent data splitting at datasets of varying sizes. For the HDGM and Sinusoid problems we use a 7:2:1 train-val-test split, and for RatInABox we use a 3:2 train-test split. Conversely, HSIC-M and HSIC-Agg use the *entire* dataset for testing. Results are shown in Figure 4. Notice that HSIC-M is able to take advantage of the additional test samples and achieves better power than some optimization-based methods at smaller datasets; however, as the size increases, optimization-based tests catch up and excel over heuristic methods. These results suggest that when the total number of samples is limited or when the dependence is straightforward, it may be advantageous to use heuristic-based tests. Conversely, if a dataset is large enough and the dependence is obscure, deep learning-based tests can be far more powerful.

**Optimizing  $J$  versus HSIC.** Rather than optimizing objective  $J$ , we can choose to maximize the test statistic HSIC; however, doing so makes no guarantees on the test power. Figure 6 compares these objectives and demonstrates that optimizing the approximate test power  $J$  is preferred over optimizing the test statistic HSIC.

## 7. Conclusion and Future Work

Kernel independence testing aims to see if two paired random variables are statistically independent given a pre-defined kernel, which is an important research line in both statistics and machine learning. As demonstrated in Figure 1 and Section 2, simple kernels as are overwhelmingly used for independence testing can be resoundingly outperformed by learned kernels tailored to a particular problem. We also, to our knowledge, are the first to propose testing based on variational mutual information estimation, which does not work quite as well as HSIC-D in our experiments but

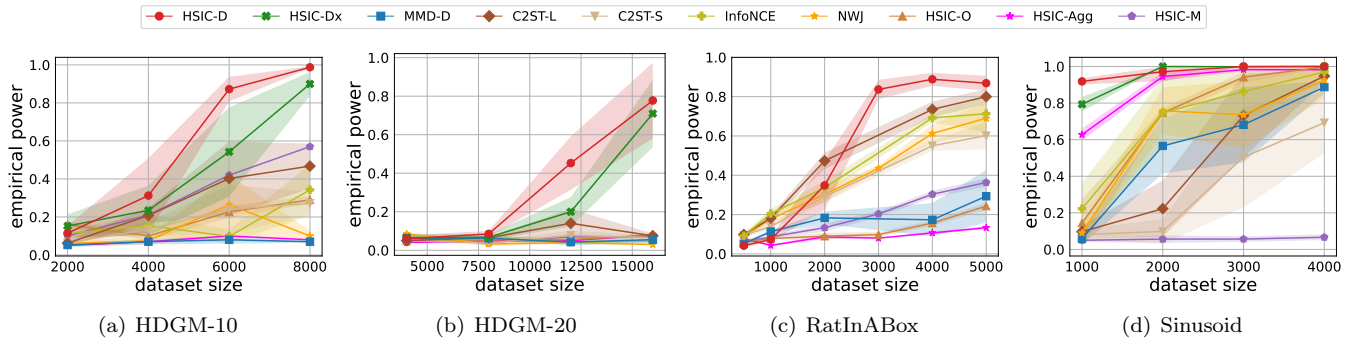


Figure 4: Empirical power vs dataset size. HDGM and Sinusoid uses a consistent 7:2:1 train-val-test split across all dataset sizes, while RatInABox maintains a 3:2 train-test split. HSIC-Agg and HSIC-M do not split the data. The shaded region covers one standard deviation over 5 training runs.

is much better than simple fixed tests. We further prove theoretically that the kernels learned HSIC-D result in powerful tests, and confirm this in experiments.

In the future, it is appealing to extend deep kernel learning schemes to conditional independence testing and apply this to causal discovery. Meanwhile, the data-splitting procedure used in this paper has to sacrifice some test power because we reduce the sample size for the final independence testing. Thus, how to make this learning scheme more data-efficient, as in HSIC-Agg (Schrab et al., 2023) or the scheme of Kübler et al. (2020); it is currently unclear, however, how to generalize this to complex data-dependent kernels.

## Acknowledgments

The authors would like to thank Roman Pogodin for productive discussions. This work was enabled in part by support provided by the Natural Sciences and Engineering Research Council of Canada, the Canada CIFAR AI Chairs program, Calcul Québec, the BC DRI Group, and the Digital Research Alliance of Canada. This work was also supported by the Australian Research Council (ARC) with grant numbers DE240101089 and DP230101540.

## References

- Arbel, Michael, Danica J. Sutherland, Mikołaj Bińkowski, and Arthur Gretton (2018). “On gradient regularizers for MMD GANs.” *NeurIPS*. arXiv: 1805.11565.
- Biau, Gérard and László Györfi (2005). “On the asymptotic properties of a nonparametric  $L_1$ -test statistic of homogeneity.” *IEEE Trans. Inf. Theory* 51.11, pp. 3965–3973.
- Blaschko, Matthew B. and Arthur Gretton (2009). “Learning Taxonomies by Dependence Maximization.” *NeurIPS*.
- Blom, Gunnar (1976). “Some Properties of Incomplete U-Statistics.” *Biometrika* 63.3, pp. 573–580.
- Bretagnolle, Jean and Catherine Huber (1978). “Estimation des densités : risque minimax.” fr. *Séminaire de probabilités de Strasbourg* 12, pp. 342–363.
- Canonne, Clément L. (2023). “A short note on an inequality between KL and TV.” arXiv: 2202.07198.
- Cheng, Xiuyuan and Alexander Cloninger (Oct. 2022). “Classification Logit Two-Sample Testing by Neural Networks for Differentiating Near Manifold Densities.” *IEEE Transactions on Information Theory* 68.10, pp. 6631–6662.
- Cucker, Felipe and Steve Smale (2002). “On the mathematical foundations of learning.” *Bulletin of the American Mathematical Society* 39.1, pp. 1–49.
- Deka, Namrata and Danica J. Sutherland (2023). “MMD-B-Fair: Learning Fair Representations with Statistical Testing.” *AISTATS*. arXiv: 2211.07907.

- Dong, Ruijiang, Feng Liu, Haoang Chi, Tongliang Liu, Mingming Gong, Gang Niu, Masashi Sugiyama, and Bo Han (2023). “Diversity-enhancing Generative Network for Few-shot Hypothesis Adaptation.” *ICML*.
- George, Tom M, Mehul Rastogi, William de Cothi, Claudia Clopath, Kimberly Stachenfeld, and Caswell Barry (Feb. 2024). “RatInABox, a toolkit for modelling locomotion and neuronal activity in continuous environments.” *eLife* 13. Ed. by Mackenzie W Mathis, Michael J Frank, and Antonio Fernandez-Ruiz, e85274.
- Gretton, Arthur, Karsten M. Borgwardt, Malte J. Rasch, Bernhard Schölkopf, and Alexander Smola (2012). “A Kernel Two-Sample Test.” *Journal of Machine Learning Research* 13.25, pp. 723–773.
- Gretton, Arthur, Olivier Bousquet, Alexander J. Smola, and Bernhard Schölkopf (2005). “Measuring Statistical Dependence with Hilbert-Schmidt Norms.” *ALT*.
- Gretton, Arthur, Bharath K. Sriperumbudur, Dino Sejdinovic, Heiko Strathmann, Sivaraman Balakrishnan, Massimiliano Pontil, and Kenji Fukumizu (2012). “Optimal kernel choice for large-scale two-sample tests.” *NeurIPS*.
- Gutmann, Michael U. and Aapo Hyvärinen (2012). “Noise-Contrastive Estimation of Unnormalized Statistical Models, with Applications to Natural Image Statistics.” *Journal of Machine Learning Research* 13.11, pp. 307–361.
- Györfi, László and I Vajda (2002). “Asymptotic distributions for goodness-of-fit statistics in a sequence of multinomial models.” *Statistics & Probability Letters* 56.1, pp. 57–67.
- Hemerik, Jesse and Jelle Goeman (2018). “Exact testing with random permutations.” *TEST* 27, pp. 811–825.
- Jean, Neal, Sang Michael Xie, and Stefano Ermon (2018). “Semi-supervised Deep Kernel Learning: Regression with Unlabeled Data by Minimizing Predictive Variance.” *NeurIPS*. arXiv: 1805.10407.
- Jitkrittum, Wittawat, Zoltán Szabó, Kacper P Chwialkowski, and Arthur Gretton (2016). “Interpretable Distribution Features with Maximum Testing Power.” *NeurIPS*.
- Kübler, Jonas M., Wittawat Jitkrittum, Bernhard Schölkopf, and Krikamol Muandet (2020). “Learning Kernel Tests Without Data Splitting.” *NeurIPS*.
- Kübler, Jonas M., Wittawat Jitkrittum, Bernhard Schölkopf, and Krikamol Muandet (2022). “A Witness Two-Sample Test.” *AISTATS*.
- Li, Chun-Liang, Wei-Cheng Chang, Yu Cheng, Yiming Yang, and Barnabás Póczos (2017). “MMD GAN: Towards Deeper Understanding of Moment Matching Network.” *NeurIPS*. arXiv: 1705.08584.
- Li, Yazhe, Roman Pogodin, Danica J. Sutherland, and Arthur Gretton (2021). “Self-Supervised Learning with Kernel Dependence Maximization.” *NeurIPS*. arXiv: 2106.08320.
- Liu, Feng, Wenkai Xu, Jie Lu, and Danica J. Sutherland (2021). “Meta Two-Sample Testing: Learning Kernels for Testing with Limited Data.” *NeurIPS*. arXiv: 2106.07636.
- Liu, Feng, Wenkai Xu, Jie Lu, Guangquan Zhang, Arthur Gretton, and Danica J. Sutherland (2020). “Learning Deep Kernels for Non-Parametric Two-Sample Tests.” *ICML*.
- Lopez-Paz, David and Maxime Oquab (2017). “Revisiting Classifier Two-Sample Tests.” *ICLR*.
- Loshchilov, Ilya and Frank Hutter (2019). “Decoupled Weight Decay Regularization.” *ICLR*. arXiv: 1711.05101.
- Lyons, Russell (2013). “Distance covariance in metric spaces.” *The Annals of Probability*.
- McAllester, David and Karl Stratos (2020). “Formal Limitations on the Measurement of Mutual Information.” *AISTATS*.
- Nguyen, XuanLong, Martin J. Wainwright, and Michael I. Jordan (Nov. 2010). “Estimating divergence functionals and the likelihood ratio by convex risk minimization.” *IEEE Trans. Inf. Theor.* 56.11, pp. 5847–5861. ISSN: 0018-9448.
- Paninski, Liam (2003). “Estimation of Entropy and Mutual Information.” *Neural Computation* 15, pp. 1191–1253.
- Poole, Ben, Sherjil Ozair, Aaron van den Oord, Alexander A. Alemi, and George Tucker (2019). “On Variational Bounds of Mutual Information.” arXiv: 1905.06922.
- Ramdas, Aaditya, Sashank J. Reddi, Barnabas Póczos, Aarti Singh, and Larry Wasserman (2015). “Adaptivity and Computation-Statistics Tradeoffs for Kernel and Distance based High Dimensional Two Sample Testing.” arXiv: 1508.00655.
- Rindt, David, Dino Sejdinovic, and David Steinsaltz (2021). “Consistency of permutation tests of independence using distance covariance, HSIC and dHSIC.” *Stat* 10.1, e364.
- Schrab, Antonin, Ilmun Kim, Benjamin Guedj, and Arthur Gretton (2023). “Efficient Aggregated Kernel Tests using Incomplete  $U$ -statistics.” arXiv: 2206.09194.
- Sejdinovic, Dino, Arthur Gretton, Bharath Sriperumbudur, and Kenji Fukumizu (2012). “Hypothesis testing using pairwise distances and associated kernels (with Appendix).” arXiv: 1205.0411 [cs.LG].

- Sejdinovic, Dino, Bharath Sriperumbudur, Arthur Gretton, and Kenji Fukumizu (2013). “Equivalence of distance-based and RKHS-based statistics in hypothesis testing.” *The Annals of Statistics*, pp. 2263–2291.
- Song, Jiaming and Stefano Ermon (2020). “Understanding the Limitations of Variational Mutual Information Estimators.” *ICLR*. arXiv: 1910.06222.
- Song, Le, Alex Smola, Arthur Gretton, Justin Bedo, and Karsten Borgwardt (2012). “Feature Selection via Dependence Maximization.” *Journal of Machine Learning Research* 13.47, pp. 1393–1434.
- Sriperumbudur, Bharath K., Kenji Fukumizu, Arthur Gretton, Bernhard Schölkopf, and Gert R. G. Lanckriet (2012). “On the empirical estimation of integral probability metrics.” *Electronic Journal of Statistics* 6, pp. 1550–1599.
- Sutherland, Danica J. and Namrata Deka (2019). “Unbiased estimators for the variance of MMD estimators.” arXiv: 1906.02104.
- Sutherland, Danica J., Hsiao-Yu Tung, Heiko Strathmann, Soumyajit De, Aaditya Ramdas, Alex Smola, and Arthur Gretton (2017). “Generative Models and Model Criticism via Optimized Maximum Mean Discrepancy.” *ICLR*.
- Szabó, Zoltán (2014). “Information Theoretical Estimators Toolbox.” *Journal of Machine Learning Research* 15.9, pp. 283–287.
- Szabó, Zoltán and Bharath K. Sriperumbudur (2018). “Characteristic and Universal Tensor Product Kernels.” *Journal of Machine Learning Research* 18.233, pp. 1–29.
- Székely, Gábor J, Maria L Rizzo, and Nail K Bakirov (2007). “Measuring and testing dependence by correlation of distances.” *The Annals of Statistics*.
- Van den Oord, Aaron, Yazhe Li, and Oriol Vinyals (2018). “Representation Learning with Contrastive Predictive Coding.” arXiv: 1807.03748.
- Wilson, Andrew Gordon, Zhiting Hu, Ruslan Salakhutdinov, and Eric P Xing (2016). “Deep kernel learning.” *AISTATS*. arXiv: 1511.02222.
- Zaremba, Wojciech, Arthur Gretton, and Matthew Blaschko (2014). “B-tests: Low Variance Kernel Two-Sample Tests.” *NeurIPS*. arXiv: 1307.1954.

## Appendix A. Uniform Convergence Analysis

### A.1 Preliminaries

We start by defining the notation used in the proofs. Let kernels  $k_\omega$  and  $l_\gamma$  be parameterized by some  $\omega$  and  $\gamma$ , and samples  $(X_i, Y_i) \sim \mathbb{P}_{xy}$  drawn i.i.d. from the joint distribution. We denote the  $n \times n$  gram matrices of  $k_\omega$  and  $l_\gamma$  by  $K^{(\omega)}$  and  $L^{(\gamma)}$  respectively. We will often omit the kernel parameters  $\omega$  and  $\gamma$  when it is clear from the context.

Let  $\eta$  be the HSIC test statistic and  $\hat{\eta}$  to be its U-statistic estimator given by

$$\hat{\eta} = \frac{1}{(n)_4} \sum_{(i,j,q,r) \in \mathbf{i}_4^n} H_{ijqr},$$

where  $(n)_k = n!/(n-k)!$  is the Pochhammer symbol and  $\mathbf{i}_4^n$  is all possible 4-tuples drawn without replacement from 1 to  $n$ .  $H$  is the kernel gram matrix of the U-statistic defined by

$$H_{ijqr} = \frac{1}{4!} \sum_{(a,b,c,d)}^{(i,j,q,r)} K_{ab} (L_{ab} + L_{cd} - 2L_{ac}),$$

where sum represents all  $4!$  combinations of tuples  $(a, b, c, d)$  that can be selected without replacement from  $(i, j, q, r)$ .

### A.2 Main Results

Our main uniform convergence results require the following assumptions.

- (A) The set of kernel parameters  $\Omega$  lies in a Banach space of dimension  $D_\Omega$ , and the set of kernel parameters  $\Gamma$  lies in a Banach space of dimension  $D_\Gamma$ . Furthermore, each parameter space is bounded by  $R_\Omega$  and  $R_\Gamma$  respectively, i.e.,

$$\begin{aligned} \Omega &\subseteq \{\omega \mid \|\omega\| \leq R_\Omega\}, \\ \Gamma &\subseteq \{\gamma \mid \|\gamma\| \leq R_\Gamma\}. \end{aligned}$$

- (B) The kernels  $k_\omega$  and  $l_\gamma$  are uniformly bounded:

$$\begin{aligned} \sup_{\omega \in \Omega} \sup_{x \in \mathcal{X}} k_\omega(x, x) &\leq \nu_k, \\ \sup_{\gamma \in \Gamma} \sup_{y \in \mathcal{Y}} l_\gamma(y, y) &\leq \nu_l. \end{aligned}$$

For the kernels we use in practice,  $\nu_k = \nu_l = 1$ .

- (C) Both kernels  $k$  and  $l$  are Lipschitz with respect to the parameter space: for all  $x, x' \in \mathcal{X}$  and  $\omega, \omega' \in \Omega$

$$|k_\omega(x, x') - k_{\omega'}(x, x')| \leq L_k \|\omega - \omega'\|,$$

and for all  $y, y' \in \mathcal{Y}$  and  $\gamma, \gamma' \in \Gamma$

$$|l_\gamma(y, y') - l_{\gamma'}(y, y')| \leq L_l \|\gamma - \gamma'\|.$$

**Theorem 6.** Under Assumptions (A) to (C), let  $\Theta \subseteq \Omega \times \Gamma$  be the set of kernel parameters  $\theta \in \Theta$  for which  $\sigma_\theta^2 \geq s^2$ , and take  $\lambda = n^{-1/3}$ . Assume  $\nu_k, \nu_l \geq 1$ . Then, with probability at least  $1 - \delta$ ,

$$\sup_{\theta \in \Theta} \left| \frac{\hat{\eta}_\theta}{\hat{\sigma}_{\theta,\lambda}} - \frac{\eta_\theta}{\sigma_\theta} \right| \leq \frac{2\nu_k\nu_l}{s^2n^{1/3}} \left[ \frac{1}{s} + \frac{9216\nu_k^2\nu_l^2}{\sqrt{n}} \right. \\ \left. + \left( 12288\nu_k^2\nu_l^2 + \frac{8s}{n^{1/6}} \right) \left( \frac{L_k}{\nu_k} + \frac{L_l}{\nu_l} + \sqrt{2 \log \frac{4}{\delta} + 2D_\Omega \log(4R_\Omega\sqrt{n}) + 2D_\Gamma \log(4R_\Gamma\sqrt{n})} \right) \right],$$

and thus, treating  $\nu_k, \nu_l$  as constants,

$$\sup_{\theta \in \Theta} \left| \frac{\hat{\eta}_\theta}{\hat{\sigma}_{\theta,\lambda}} - \frac{\eta_\theta}{\sigma_\theta} \right| = \tilde{\mathcal{O}}_P \left( \frac{1}{s^2n^{1/3}} \left[ \frac{1}{s} + L_k + L_l + \sqrt{D_\Omega} + \sqrt{D_\Gamma} \right] \right).$$

*Proof.* Let  $\hat{\sigma}_{\theta,\lambda}^2 := \hat{\sigma}_\theta^2 + \lambda$  be our regularized variance estimator from which we can assume is positive. We start by decomposing

$$\begin{aligned} \sup_{\theta \in \Theta} \left| \frac{\hat{\eta}_\theta}{\hat{\sigma}_{\theta,\lambda}} - \frac{\eta_\theta}{\sigma_\theta} \right| &\leq \sup_{\theta \in \Theta} \left| \frac{\hat{\eta}_\theta}{\hat{\sigma}_{\theta,\lambda}} - \frac{\hat{\eta}_\theta}{\sigma_{\theta,\lambda}} \right| + \sup_{\theta \in \Theta} \left| \frac{\hat{\eta}_\theta}{\sigma_{\theta,\lambda}} - \frac{\hat{\eta}_\theta}{\sigma_\theta} \right| + \sup_{\theta \in \Theta} \left| \frac{\hat{\eta}_\theta}{\sigma_\theta} - \frac{\eta_\theta}{\sigma_\theta} \right| \\ &= \sup_{\theta} \frac{|\hat{\eta}_\theta|}{\hat{\sigma}_{\theta,\lambda} \cdot \sigma_{\theta,\lambda}} \frac{|\hat{\sigma}_{\theta,\lambda}^2 - \sigma_{\theta,\lambda}^2|}{\hat{\sigma}_{\theta,\lambda} + \sigma_{\theta,\lambda}} + \sup_{\theta} \frac{|\hat{\eta}_\theta|}{\sigma_{\theta,\lambda} \cdot \sigma_\theta} \frac{|\sigma_{\theta,\lambda}^2 - \sigma_\theta^2|}{\sigma_{\theta,\lambda} + \sigma_\theta} + \sup_{\theta} \frac{1}{\sigma_\theta} |\hat{\eta}_\theta - \eta_\theta| \\ &\leq \frac{4\nu_k\nu_l}{s\sqrt{\lambda}(s + \sqrt{\lambda})} \sup_{\theta} |\hat{\sigma}_\theta^2 - \sigma_\theta^2| + \frac{4\nu_k\nu_l\lambda}{s\sqrt{s^2 + \lambda}(s + \sqrt{s^2 + \lambda})} + \frac{1}{s} \sup_{\theta} |\hat{\eta}_\theta - \eta_\theta| \\ &\leq \frac{4\nu_k\nu_l}{s^2\sqrt{\lambda}} \sup_{\theta} |\hat{\sigma}_\theta^2 - \sigma_\theta^2| + \frac{1}{s} \sup_{\theta} |\hat{\eta}_\theta - \eta_\theta| + \frac{2\nu_k\nu_l\lambda}{s^3}. \end{aligned}$$

Proposition 7 and Proposition 8 show the uniform convergence of  $\hat{\eta}_\theta$  and  $\hat{\sigma}_\theta$ , from which we get that with probability at least  $1 - \delta$ , the error is at most

$$\begin{aligned} \sup_{\theta \in \Theta} \left| \frac{\hat{\eta}_\theta}{\hat{\sigma}_{\theta,\lambda}} - \frac{\eta_\theta}{\sigma_\theta} \right| &\leq \frac{2\nu_k\nu_l\lambda}{s^3} + \frac{18432\nu_k^3\nu_l^3}{s^2n\sqrt{\lambda}} + \left[ \frac{8192\nu_k^3\nu_l^3}{s^2\sqrt{\lambda n}} + \frac{8\nu_k\nu_l}{s\sqrt{n}} \right] \left( \frac{L_k}{\nu_k} + \frac{L_l}{\nu_l} \right) \\ &\quad + \left[ \frac{24576\nu_k^3\nu_l^3}{s^2\sqrt{\lambda n}} + \frac{16\nu_k\nu_l}{s\sqrt{n}} \right] \sqrt{2 \log \frac{4}{\delta} + 2D_\Omega \log(4R_\Omega\sqrt{n}) + 2D_\Gamma \log(4R_\Gamma\sqrt{n})}. \end{aligned}$$

Taking  $\lambda = n^{-1/3}$  gives

$$\begin{aligned} \sup_{\theta \in \Theta} \left| \frac{\hat{\eta}_\theta}{\hat{\sigma}_{\theta,\lambda}} - \frac{\eta_\theta}{\sigma_\theta} \right| &\leq \frac{2\nu_k\nu_l}{s^3n^{1/3}} + \frac{18432\nu_k^3\nu_l^3}{s^2n^{5/6}} + \left[ \frac{8192\nu_k^3\nu_l^3}{s^2n^{1/3}} + \frac{8\nu_k\nu_l}{s\sqrt{n}} \right] \left( \frac{L_k}{\nu_k} + \frac{L_l}{\nu_l} \right) \\ &\quad + \left[ \frac{24576\nu_k^3\nu_l^3}{s^2n^{1/3}} + \frac{16\nu_k\nu_l}{s\sqrt{n}} \right] \sqrt{2 \log \frac{4}{\delta} + 2D_\Omega \log(4R_\Omega\sqrt{n}) + 2D_\Gamma \log(4R_\Gamma\sqrt{n})}. \end{aligned}$$

Using  $\nu_k, \nu_l \geq 1$  we can slightly simplify our bound to

$$\begin{aligned} \sup_{\theta \in \Theta} \left| \frac{\hat{\eta}_\theta}{\hat{\sigma}_{\theta,\lambda}} - \frac{\eta_\theta}{\sigma_\theta} \right| &\leq \left[ \frac{24576\nu_k^3\nu_l^3}{s^2n^{1/3}} + \frac{16\nu_k\nu_l}{s\sqrt{n}} \right] \left( \frac{L_k}{\nu_k} + \frac{L_l}{\nu_l} + \sqrt{2 \log \frac{4}{\delta} + 2D_\Omega \log(4R_\Omega\sqrt{n}) + 2D_\Gamma \log(4R_\Gamma\sqrt{n})} \right) \\ &\quad + \frac{2\nu_k\nu_l}{s^3n^{1/3}} + \frac{18432\nu_k^3\nu_l^3}{s^2n^{5/6}} \end{aligned}$$

□

### A.3 Uniform convergence results

This subsection pertains to uniform convergence results of  $\hat{\eta}_\theta$  and  $\hat{\sigma}_\theta$ , and are used in the proof of Theorem 6.

**Proposition 7.** *Under assumptions (A) to (C), we have that with probability at least  $1 - \delta$ ,*

$$\sup_{\theta \in \Theta} |\hat{\eta}_\theta - \eta_\theta| \leq \frac{8\nu_k \nu_l}{\sqrt{n}} \left( \frac{L_k}{\nu_k} + \frac{L_l}{\nu_l} + 2\sqrt{2 \log \frac{2}{\delta} + 2D_\Omega \log(4R_\Omega \sqrt{n}) + 2D_\Gamma \log(4R_\Gamma \sqrt{n})} \right).$$

*Proof.* We use  $\epsilon$ -net arguments on both spaces  $\Omega$  and  $\Gamma$ . Let  $\{\omega_i\}_{i=1}^{T_\Omega}$  be arbitrarily placed centers with radius  $\rho_\Omega$  such that any point  $\omega \in \Omega$  satisfies  $\min \|\omega - \omega_i\| \leq \rho_\Omega$ . Similarly, let  $\{\gamma_i\}_{i=1}^{T_\Gamma}$  be centers with radius  $\rho_\Gamma$  satisfying  $\min \|\gamma - \gamma_i\| \leq \rho_\Gamma$  for any  $\gamma \in \Gamma$ . Assumption (B) ensures this is possible with at most  $T_\Omega = (4R_\Omega/\rho_\Omega)^{D_\Omega}$  and  $T_\Gamma = (4R_\Gamma/\rho_\Gamma)^{D_\Gamma}$  points respectively (Cucker and Smale, 2002, Proposition 5).

We can decompose the convergence bound into simpler components and tackle each component individually

$$\sup_{\theta \in \Theta} |\hat{\eta}_\theta - \eta_\theta| \leq \sup_{\theta} |\hat{\eta}_\theta - \hat{\eta}_{\theta'}| + \max_{\substack{\omega' \in \{\omega_1, \dots, \omega_{T_\Omega}\} \\ \gamma' \in \{\gamma_1, \dots, \gamma_{T_\Gamma}\}}} |\hat{\eta}_{\theta'} - \eta_{\theta'}| + \sup_{\theta} |\eta_{\theta'} - \eta_\theta|.$$

First, let us analyze  $|\eta_\theta - \eta_{\theta'}|$  for any  $\theta, \theta' \in \Theta$ . Recall that  $\eta = \mathbb{E}[H_{1234}]$  where  $H_{1234} = \frac{1}{4!} \sum_{(a,b,c,d)}^{(1,2,3,4)} K_{ab}(L_{ab} + L_{cd} - 2L_{ac})$ . We have that

$$\begin{aligned} |H_{1234}^{(\theta)} - H_{1234}^{(\theta')}| &\leq \frac{1}{4!} \sum_{(abcd)}^{(1234)} \left| K_{ab}^{(\omega)}(L_{ab}^{(\gamma)} + L_{cd}^{(\gamma)} - 2L_{ac}^{(\gamma)}) - K_{ab}^{(\omega')} (L_{ab}^{(\gamma')} + L_{cd}^{(\gamma')} - 2L_{ac}^{(\gamma')}) \right| \\ &\leq \frac{1}{4!} \sum_{(abcd)}^{(1234)} \left( \left| K_{ab}^{(\omega)} L_{ab}^{(\gamma)} - K_{ab}^{(\omega')} L_{ab}^{(\gamma')} \right| + \left| K_{ab}^{(\omega)} L_{cd}^{(\gamma)} - K_{ab}^{(\omega')} L_{cd}^{(\gamma')} \right| + 2 \left| K_{ab}^{(\omega')} L_{ac}^{(\gamma')} - K_{ab}^{(\omega)} L_{ac}^{(\gamma)} \right| \right). \end{aligned}$$

From Assumption (A) we know that  $|K_{ab}| \leq \nu_k$  and  $|L_{ab}| \leq \nu_l$ , and via Assumption (C) we notice that

$$\begin{aligned} \left| K_{ab}^{(\omega)} L_{ab}^{(\gamma)} - K_{ab}^{(\omega')} L_{ab}^{(\gamma')} \right| &= \left| K_{ab}^{(\omega)} L_{ab}^{(\gamma)} - K_{ab}^{(\omega)} L_{ab}^{(\gamma')} + K_{ab}^{(\omega)} L_{ab}^{(\gamma')} - K_{ab}^{(\omega')} L_{ab}^{(\gamma')} \right| \\ &\leq \left| K_{ab}^{(\omega)} \right| \left| L_{ab}^{(\gamma)} - L_{ab}^{(\gamma')} \right| + \left| L_{ab}^{(\gamma')} \right| \left| K_{ab}^{(\omega)} - K_{ab}^{(\omega')} \right| \\ &\leq \nu_k L_l \|v - v'\| + \nu_l L_k \|\omega - \omega'\| \\ &\leq \nu_k L_l \rho_\Gamma + \nu_l L_k \rho_\Omega. \end{aligned}$$

This expression is true for all three components of  $|H_{1234}^{(\theta)} - H_{1234}^{(\theta')}|$  and so it follows that

$$\begin{aligned} |\eta_\theta - \eta_{\theta'}| &= \left| \mathbb{E}[H_{1234}^{(\theta)}] - \mathbb{E}[H_{1234}^{(\theta')}] \right| \leq \mathbb{E} \left| H_{1234}^{(\theta)} - H_{1234}^{(\theta')} \right| \leq 4\nu_k L_l \rho_\Gamma + 4\nu_l L_k \rho_\Omega, \\ |\hat{\eta}_\theta - \hat{\eta}_{\theta'}| &= \left| \frac{1}{(n)_4} \sum_{(i,j,q,r) \in \mathbf{i}_4^n} H_{ijqr}^{(\theta)} - H_{ijqr}^{(\theta')} \right| \leq \frac{1}{(n)_4} \sum_{(i,j,q,r) \in \mathbf{i}_4^n} \left| H_{1234}^{(\theta)} - H_{1234}^{(\theta')} \right| \leq 4\nu_k L_l \rho_\Gamma + 4\nu_l L_k \rho_\Omega. \end{aligned}$$

Now, we study the random error function  $\Delta := \hat{\eta} - \eta$ . Note that  $\mathbb{E} \Delta = 0$  since  $\hat{\eta}$  is unbiased, and  $|H_{ijqr}| \leq 4\nu_k \nu_l$  via Assumption (A). This  $\hat{\eta}$ , and hence  $\Delta$ , satisfies bounded differences. Let  $F$  denote the kernel tensor  $H$  but with sample  $(X_\ell, Y_\ell)$  replaced by  $(X'_\ell, Y'_\ell)$  so that  $F$  agrees with  $H$  except at indices  $\ell$ , and let  $\hat{\eta}' = \frac{1}{(n)_4} \sum_{(i,j,q,r) \in \mathbf{i}_4^n} F_{ijqr}$  be it's HSIC estimator.



For convenience, we denote  $(i, j, q, r) \in \mathbf{i}_4^n$  simply as  $(i, j, q, r)$ , and  $(i, j, q) \setminus k$  to be the set of 3-tuples drawn without replacement from  $\mathbf{i}_3^n$  that exclude the number  $k$ . We can compute the maximal bounded difference  $|\Delta - \Delta'| = |\hat{\eta} - \hat{\eta}'|$  as

$$\begin{aligned} |\hat{\eta} - \hat{\eta}'| &= \left| \frac{1}{(n)_4} \sum_{(i,j,q,r)} H_{ijqr} - F_{ijqr} \right| \leq \frac{1}{(n)_4} \sum_{(i,j,q,r)} |H_{ijqr} - F_{ijqr}| \\ &= \frac{1}{(n)_4} \left( \sum_{(j,q,r) \setminus \ell} \underbrace{|H_{\ell jqr} - F_{\ell jqr}|}_{\leq 8\nu_k \nu_l} + \sum_{(i,q,r) \setminus \ell} |H_{i\ell qr} - F_{i\ell qr}| + \sum_{(i,j,r) \setminus \ell} |H_{ij\ell r} - F_{ij\ell r}| + \sum_{(i,j,q) \setminus \ell} |H_{ijq\ell} - F_{ijq\ell}| \right) \\ &= \frac{1}{(n)_4} \left( (n-1)_3 \cdot 8\nu_k \nu_l \cdot 4 \right) = \frac{32\nu_k \nu_l}{n}. \end{aligned} \tag{10}$$

Then, applying McDiarmid's inequality on  $\Delta := \hat{\eta} - \eta$  followed by a union bound over the  $T_\Omega T_\Gamma$  center pairs gives us, with probability at least  $1 - \delta$ , that

$$\begin{aligned} \max_{\substack{\omega' \in \{\omega_1, \dots, \omega_{T_\Omega}\} \\ \gamma' \in \{\gamma_1, \dots, \gamma_{T_\Gamma}\}}} |\hat{\eta}_{\theta'} - \eta_{\theta'}| &\leq 32\nu_k \nu_l \sqrt{\frac{1}{2n} \log \frac{2T_\Omega T_\Gamma}{\delta}} \\ &= \frac{16\nu_k \nu_l}{\sqrt{n}} \sqrt{2 \log \frac{2}{\delta} + 2 \log T_\Omega + 2 \log T_\Gamma} \\ &= \frac{16\nu_k \nu_l}{\sqrt{n}} \sqrt{2 \log \frac{2}{\delta} + 2D_\Omega \log \frac{4R_\Omega}{\rho_\Omega} + 2D_\Gamma \log \frac{4R_\Gamma}{\rho_\Gamma}}. \end{aligned}$$

Finally, we combine these results to get our uniform convergence bound:

$$\begin{aligned} \sup_{\theta \in \Theta} |\hat{\eta}_\theta - \eta_\theta| &\leq 8\nu_k L_l \rho_\Gamma + 8\nu_l L_k \rho_\Omega + \frac{16\nu_k \nu_l}{\sqrt{n}} \sqrt{2 \log \frac{2}{\delta} + 2D_\Omega \log \frac{4R_\Omega}{\rho_\Omega} + 2D_\Gamma \log \frac{4R_\Gamma}{\rho_\Gamma}} \\ &= 8\nu_k \nu_l \left( \frac{L_k}{\nu_k} \rho_\Omega + \frac{L_l}{\nu_l} \rho_\Gamma + \frac{2}{\sqrt{n}} \sqrt{2 \log \frac{2}{\delta} + 2D_\Omega \log \frac{4R_\Omega}{\rho_\Omega} + 2D_\Gamma \log \frac{4R_\Gamma}{\rho_\Gamma}} \right). \end{aligned}$$

Setting  $\rho_\Omega = \rho_\Gamma = 1/\sqrt{n}$  yields the desired result.  $\square$

**Proposition 8.** *Under assumptions (A) to (C), we have that with probability at least  $1 - \delta$ ,*

$$\sup_{\theta \in \Theta} |\hat{\sigma}_\theta^2 - \sigma_\theta^2| \leq \frac{2048\nu_k^2 \nu_l^2}{\sqrt{n}} \left( \frac{L_k}{\nu_k} + \frac{L_l}{\nu_l} + 3 \sqrt{2 \log \frac{2}{\delta} + 2D_\Omega \log(4R_\Omega \sqrt{n}) + 2D_\Gamma \log(4R_\Gamma \sqrt{n})} + \frac{9}{4\sqrt{n}} \right).$$

*Proof.* We use an  $\epsilon$ -net argument on both spaces  $\Omega$  and  $\Gamma$ . Using the same construction as in Proposition 7, we once again decompose our convergence bound:

$$\sup_{\theta \in \Theta} |\hat{\sigma}_\theta^2 - \sigma_\theta^2| \leq \sup_{\theta} |\hat{\sigma}_\theta^2 - \hat{\sigma}_{\theta'}^2| + \max_{\substack{\omega' \in \{\omega_1, \dots, \omega_{T_\Omega}\} \\ \gamma' \in \{\gamma_1, \dots, \gamma_{T_\Gamma}\}}} |\hat{\sigma}_{\theta'}^2 - \sigma_{\theta'}^2| + \sup_{\theta} |\sigma_\theta^2 - \sigma_{\theta'}^2|.$$

First, let us analyze  $|\sigma_\theta^2 - \sigma_{\theta'}^2|$  for any  $\theta, \theta' \in \Theta$ . Recall that  $\sigma^2 = 16 (\mathbb{E}[H_{1234}H_{1567}] - \eta^2)$ . It follows that

$$\begin{aligned} |\sigma_\theta^2 - \sigma_{\theta'}^2| &= 16 \left| \mathbb{E}[H_{1234}^{(\theta)} H_{1567}^{(\theta)}] - H_{1234}^{(\theta')} H_{1567}^{(\theta')} \right] - \mathbb{E}[H_{1234}^{(\theta)} H_{5678}^{(\theta)}] + \mathbb{E}[H_{1234}^{(\theta')} H_{5678}^{(\theta')}] \Big| \\ &\leq 16 \mathbb{E} \left| H_{1234}^{(\theta)} H_{1567}^{(\theta)} - H_{1234}^{(\theta')} H_{1567}^{(\theta')} \right| + 16 \mathbb{E} \left| H_{1234}^{(\theta)} H_{5678}^{(\theta)} - H_{1234}^{(\theta')} H_{5678}^{(\theta')} \right|. \end{aligned}$$

Under Assumptions (A) and (C) we know that  $|H_{1234}| \leq 4\nu_k\nu_l$  and  $|H_{1234}^{(\theta)} - H_{1234}^{(\theta')}| \leq 4\nu_k L_l \rho_\Gamma + 4\nu_l L_k \rho_\Omega$ . As such, we have

$$\begin{aligned} |H_{1234}^{(\theta)} H_{1567}^{(\theta)} - H_{1234}^{(\theta')} H_{1567}^{(\theta')}| &\leq |H_{1234}^{(\theta)} H_{1567}^{(\theta)} - H_{1234}^{(\theta)} H_{1567}^{(\theta')}| + |H_{1234}^{(\theta)} H_{1567}^{(\theta')} - H_{1234}^{(\theta')} H_{1567}^{(\theta')}| \\ &= |H_{1234}^{(\theta)}| |H_{1567}^{(\theta)} - H_{1567}^{(\theta')}| + |H_{1567}^{(\theta')}| |H_{1234}^{(\theta)} - H_{1234}^{(\theta')}| \\ &\leq 32\nu_k\nu_l(\nu_k L_l \rho_\Gamma + \nu_l L_k \rho_\Omega) \end{aligned}$$

This expression is true for both components of  $|\sigma_\theta^2 - \sigma_{\theta'}^2|$  and so it follows that

$$|\sigma_\theta^2 - \sigma_{\theta'}^2| \leq 1024\nu_k\nu_l(\nu_k L_l \rho_\Gamma + \nu_l L_k \rho_\Omega). \quad (11)$$

Similarly, replacing the expectations  $\mathbb{E}[H_{1234}H_{1567}]$  and  $\mathbb{E}[H_{1234}H_{5678}]$  with the respective estimators  $\frac{1}{(n)_4(n-1)_3} \sum_{(ijqr),(bcd)\setminus i} H_{ijqr}H_{ibcd}$  and  $\frac{1}{(n)_4} \sum_{(ijqr),(abcd)} H_{ijqr}H_{abcd}$  give us the same bound

$$|\hat{\sigma}_\theta^2 - \hat{\sigma}_{\theta'}^2| \leq 1024\nu_k\nu_l(\nu_k L_l \rho_\Gamma + \nu_l L_k \rho_\Omega). \quad (12)$$

Next, using Lemma 9 and Lemma 10 followed by a union bound over the  $T_\Omega T_\Gamma$  center combinations gives us, with probability at least  $1 - \delta$ ,

$$\begin{aligned} \max_{\substack{\omega' \in \{\omega_1, \dots, \omega_{T_\Omega}\} \\ \gamma' \in \{\gamma_1, \dots, \gamma_{T_\Gamma}\}}} |\hat{\sigma}_{\theta'}^2 - \sigma_{\theta'}^2| &\leq 6144\nu_k^2\nu_l^2 \sqrt{\frac{2}{n} \log \frac{2T_\Omega T_\Gamma}{\delta}} + \frac{4608\nu_k^2\nu_l^2}{n} \\ &\leq \frac{2048\nu_k^2\nu_l^2}{\sqrt{n}} \left( 3\sqrt{2 \log \frac{2}{\delta} + 2D_\Omega \log \frac{4R_\Omega}{\rho_\Omega} + 2D_\Gamma \log \frac{4R_\Gamma}{\rho_\Gamma} + \frac{9}{4\sqrt{n}}} \right). \end{aligned} \quad (13)$$

Finally, we combine Equations (11) to (13) to get

$$\sup_{\theta \in \Theta} |\hat{\sigma}_\theta^2 - \sigma_\theta^2| \leq \frac{2048\nu_k^2\nu_l^2}{\sqrt{n}} \left( 3\sqrt{2 \log \frac{2}{\delta} + 2D_\Omega \log \frac{4R_\Omega}{\rho_\Omega} + 2D_\Gamma \log \frac{4R_\Gamma}{\rho_\Gamma} + \frac{9}{4\sqrt{n}}} + \sqrt{n} \left( \frac{L_k}{\nu_k} \rho_\Omega + \frac{L_l}{\nu_l} \rho_\Gamma \right) \right).$$

Setting  $\rho_\Omega = \rho_\Gamma = 1/\sqrt{n}$  gives us our desired uniform convergence bound.  $\square$

**Lemma 9.** *For any kernels  $k$  and  $l$  satisfying Assumption (A), with probability at least  $1 - \delta$  we have*

$$|\hat{\sigma}^2 - \mathbb{E} \hat{\sigma}^2| \leq 6144\nu_k^2\nu_l^2 \sqrt{\frac{2}{n} \log \frac{2}{\delta}}.$$

*Proof.* We apply McDiarmid's inequality to  $\hat{\sigma}^2$ . First, we show that the variance estimator satisfies bounded differences. For convenience, we denote  $(i, j, q, r) \in \mathbf{i}_4^n$  simply as  $(i, j, q, r)$ , and  $(i, j, q) \setminus k$  to be the set of 3-tuples drawn without replacement from  $\mathbf{i}_3^n$  that exclude the number  $k$ . Recall that

$$\hat{\sigma}^2 = 16 \left( \frac{1}{(n)_4(n-1)_3} \sum_{\substack{(i,j,q,r) \\ (b,c,d)\setminus i}} H_{ijqr}H_{ibcd} - \hat{\eta}^2 \right).$$

Let  $F$  denote the kernel tensor  $H$  but with sample  $(X_\ell, Y_\ell)$  replaced by  $(X'_\ell, Y'_\ell)$  so that  $F$  agrees with  $H$  except at indices  $\ell$ , and let  $\hat{\eta}'$  and  $\hat{\sigma}'^2$  denote the HSIC and its variance estimators according to this updated sample set. The deviation is then

$$|\hat{\sigma}^2 - \hat{\sigma}'^2| \leq \frac{16}{(n)_4(n-1)_3} \sum_{\substack{(i,j,q,r) \\ (b,c,d)\setminus i}} |H_{ijqr}H_{ibcd} - F_{ijqr}F_{ibcd}| + 16|\hat{\eta}^2 - \hat{\eta}'^2|.$$

We bound the first term by noticing that  $\Delta := H_{ijqr}H_{ibcd} - F_{ijqr}F_{ibcd}$  is zero when none of the indices  $\{i, j, q, r, b, c, d\}$  is  $\ell$ . Let  $S := \{(i, j, q, r, b, c, d) : (i, j, q, r) \in \mathbf{i}_4^n, (b, c, d) \in \mathbf{i}_3^n \setminus \{i\}, \ell \in \{i, j, q, r, b, c, d\}\}$  be the set of indices where  $\Delta$  may be non-zero. By Assumption (A) we know that  $|\Delta| \leq 32\nu_k^2\nu_l^2$ . Thus, we can bound the first term by

$$\begin{aligned} \frac{16}{(n)_4(n-1)_3} \sum_S |\Delta| &= \frac{512\nu_k^2\nu_l^2}{(n)_4(n-1)_3} |S| \\ &= \frac{512\nu_k^2\nu_l^2}{(n)_4(n-1)_3} \left[ \underbrace{4(n-1)_3^2}_{\ell \in \{i, j, q, r\}} + \underbrace{3(n-1)(n-2)_2(n-1)_3}_{\ell \in \{b, c, d\}} - \underbrace{9(n-1)_3(n-2)_2}_{\ell \in \{j, q, r\} \text{ and } \ell \in \{b, c, d\}} \right] \\ &= 512\nu_k^2\nu_l^2 \left( \frac{16}{n} - \frac{9}{n-1} \right) \\ &\leq \frac{8192\nu_k^2\nu_l^2}{n} \quad (\forall n > 1). \end{aligned}$$

We can bound the second term using  $|\hat{\eta}| \leq 4\nu_k\nu_l$  (Assumption (A)) and the bounded difference result (10) from Proposition 7:

$$16|\hat{\eta}^2 - \hat{\eta}'^2| = 16|\hat{\eta} + \hat{\eta}'||\hat{\eta} - \hat{\eta}'| \leq 16 \cdot 8\nu_k\nu_l \cdot \frac{32\nu_k\nu_l}{n} = \frac{4096\nu_k^2\nu_l^2}{n}.$$

Combining these two terms, the maximal bounded difference for  $\hat{\sigma}^2$  is

$$|\hat{\sigma}^2 - \hat{\sigma}'^2| \leq \frac{12288\nu_k^2\nu_l^2}{n}.$$

Finally, applying McDiarmid's inequality gives us, with probability at least  $1 - \delta$ ,

$$|\hat{\sigma}^2 - \mathbb{E} \hat{\sigma}^2| \leq 6144\nu_k^2\nu_l^2 \sqrt{\frac{2}{n} \log \frac{2}{\delta}}.$$

□

**Lemma 10.** *For any kernels  $k$  and  $l$  satisfying Assumption (A), the bias is bounded by*

$$|\mathbb{E} \hat{\sigma}^2 - \sigma^2| \leq \frac{4608\nu_k^2\nu_l^2}{n}.$$

*Proof.* The expectation of the variance estimator is

$$\mathbb{E} \hat{\sigma}^2 = 16 \left( \frac{1}{(n)_4(n-1)_3} \sum_{\substack{(i, j, q, r) \\ (b, c, d) \setminus i}} \mathbb{E}[H_{ijqr}H_{ibcd}] - \frac{1}{(n)_4} \sum_{\substack{(i, j, q, r) \\ (a, b, c, d)}} \mathbb{E}[H_{ijqr}H_{abcd}] \right).$$

First, we can break down the left-hand sum into only terms of  $\mathbb{E}[H_{1234}H_{1567}]$  by considering the cases where  $\{i, j, q, r, b, c, d\}$  are unique. Let  $S = \{(i, j, q, r, b, c, d) : (i, j, q, r) \in \mathbf{i}_4^n, (b, c, d) \in \mathbf{i}_3^n \setminus \{i\}\}$  be the set of all possible indices of our left-hand sum. It follows that

$$\sum_S \mathbb{E}[H_{ijqr}H_{ibcd}] = \sum_{(i, j, q, r, b, c, d) \in \mathbf{i}_7^n} \mathbb{E}[H_{ijqr}H_{ibcd}] + \sum_{S \setminus \mathbf{i}_7^n} \mathbb{E}[H_{ijqr}H_{ibcd}].$$

If all indices are unique, then the expectation  $\mathbb{E}[H_{ijqr}H_{ibcd}]$  is equivalent to  $\mathbb{E}[H_{1234}H_{1567}]$ ; otherwise, we can bound the expectation by  $16\nu_k^2\nu_l^2$  via Assumption (A). Thus, the bound on the left-hand sum is

$$\sum_{\substack{(i,j,q,r) \\ (b,c,d)\setminus i}} \mathbb{E}[H_{ijqr}H_{ibcd}] \leq (n)_7 \mathbb{E}[H_{1234}H_{1567}] + \left( (n)_4(n-1)_3 - (n)_7 \right) 16\nu_k^2\nu_l^2.$$

Similarly, we can break down the right-hand sum into only terms of  $\mathbb{E}[H_{1234}H_{5678}]$ . Let  $R = \{(i, j, q, r, a, b, c, d) : (i, j, q, r) \in \mathbf{i}_4^n, (a, b, c, d) \in \mathbf{i}_4^n\}$  be the possible indices of our right-hand sum. We have that

$$\begin{aligned} \sum_{\substack{(i,j,q,r) \\ (a,b,c,d)}} \mathbb{E}[H_{ijqr}H_{abcd}] &= \sum_{(i,j,q,r,a,b,c,d) \in \mathbf{i}_8^n} \mathbb{E}[H_{ijqr}H_{abcd}] + \sum_{R \setminus \mathbf{i}_8^n} \mathbb{E}[H_{ijqr}H_{abcd}] \\ &\leq (n)_8 \mathbb{E}[H_{1234}H_{5678}] + \left( (n)_4^2 - (n)_8 \right) 16\nu_k^2\nu_l^2. \end{aligned}$$

Now, using these two results and Assumption (A), we can compute a bound on the desired bias of  $\hat{\sigma}^2$ :

$$\begin{aligned} |\mathbb{E} \hat{\sigma}^2 - \sigma^2| &= 16 \left| \frac{1}{(n)_4(n-1)_3} \sum_{\substack{(i,j,q,r) \\ (b,c,d)\setminus i}} \mathbb{E}[H_{ijqr}H_{ibcd}] - \mathbb{E}[H_{1234}H_{1567}] - \frac{1}{(n)_4^2} \sum_{\substack{(i,j,q,r) \\ (a,b,c,d)}} \mathbb{E}[H_{ijqr}H_{abcd}] + \mathbb{E}[H_{1234}H_{5678}] \right| \\ &\leq 16 \left| \left( 1 - \frac{(n)_7}{(n)_4(n-1)_3} \right) \left( 16\nu_k^2\nu_l^2 - \underbrace{\mathbb{E}[H_{1234}H_{1567}]}_{-16\nu_k^2\nu_l^2 \leq \cdot \leq 16\nu_k^2\nu_l^2} \right) + \left( 1 - \frac{(n)_8}{(n)_4^2} \right) \left( \underbrace{\mathbb{E}[H_{1234}H_{5678}]}_{0 \leq \cdot \leq 16\nu_k^2\nu_l^2} - 16\nu_k^2\nu_l^2 \right) \right| \\ &\leq 16 \left( 1 - \frac{(n)_7}{(n)_4(n-1)_3} \right) 32\nu_k^2\nu_l^2 < 512\nu_k^2\nu_l^2 \cdot \frac{9}{n} \quad (\forall n \geq 4) \\ &= \frac{4608\nu_k^2\nu_l^2}{n}. \end{aligned} \quad \square$$

## Appendix B. Additional Experiments

### B.1 High-Dimensional Gaussian Mixture

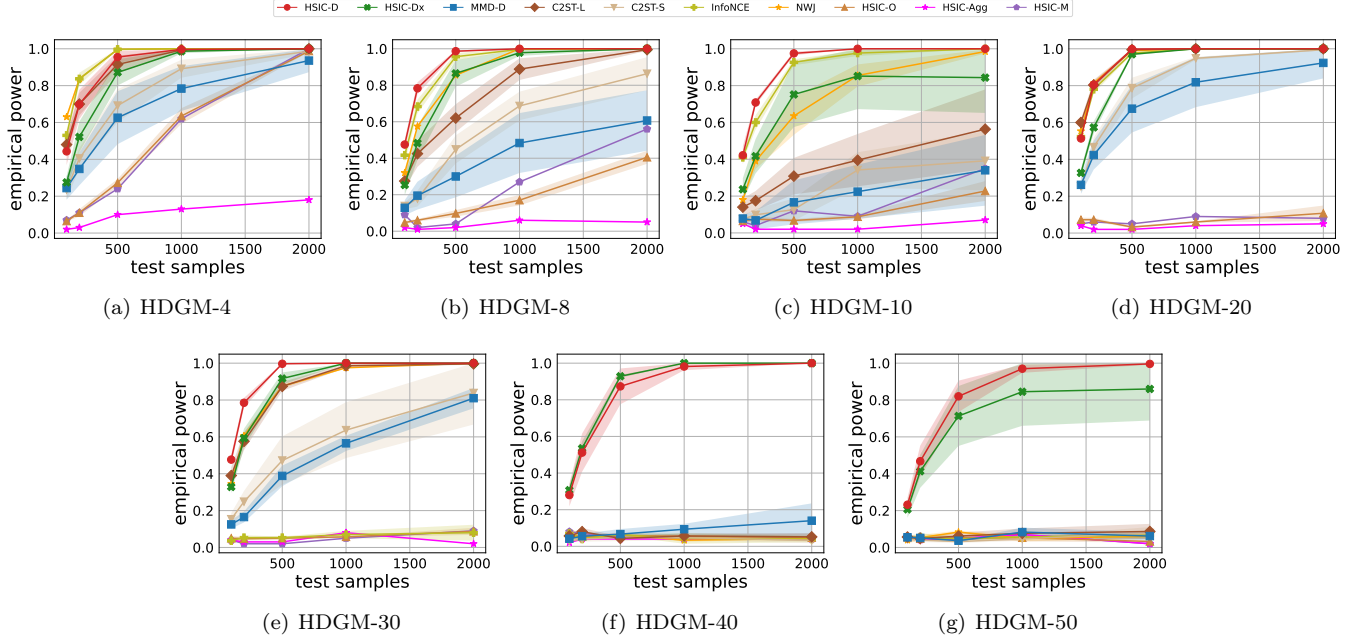


Figure 5: Empirical power vs test size for the HDGM problem at dimensions  $d = \{2, 4, 5, 10, 15, 20\}$ . The average test power is computed over 5 training instances and the shaded region covers one standard error from the mean.

### B.2 Type-I Error

Table 1 shows that the type-I error rates for our optimization-based tests are well-controlled.

Method	HDGM-4	HDGM-8	HDGM-10	HDGM-20	HDGM-30	HDGM-40	HDGM-50	Sinusoid	RatInABox
HSIC-D	0.043	0.043	0.050	0.050	0.062	0.057	0.052	0.050	0.048
MMD-D	0.048	0.055	0.040	0.053	0.048	0.048	0.055	0.054	0.050
C2ST-L	0.060	0.030	0.053	0.048	0.053	0.058	0.045	0.046	0.048
InfoNCE	0.046	0.046	0.046	0.054	0.044	0.050	0.048	0.048	0.045
NWJ	0.050	0.054	0.058	0.052	0.044	0.064	0.054	0.052	0.042

Table 1: Average type-I error rates under the null distribution over 400 tests. We use  $m = 512$  samples.

### B.3 Optimizing $J$ vs. HSIC

We examine the trade-off between optimizing the approximate test power  $J$  versus just the test statistic HSIC. The results on power versus test size are show in Figure 6. Optimizing our proposed objective  $J$  significantly outperforms optimizing HSIC for all problems.

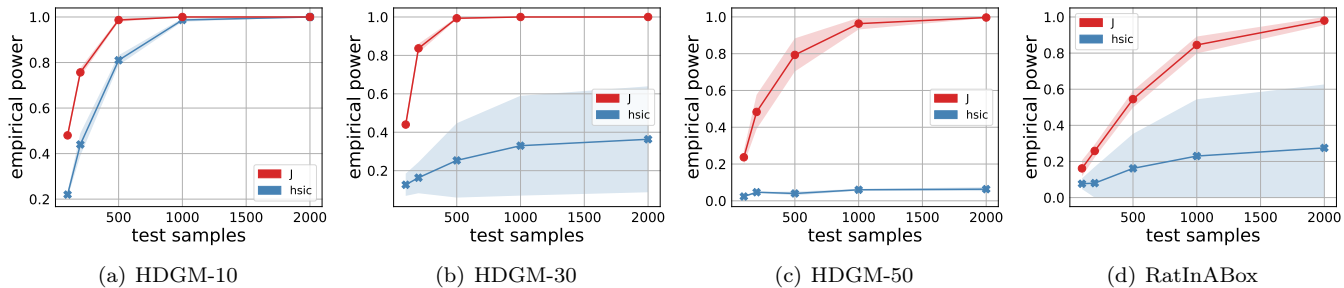


Figure 6: Test power using deep kernels optimized for the approximate asymptotic test power  $J$  (red) versus optimizing just the test statistic HSIC (blue).

### B.4 Asymptotic Variance: HSIC vs. MMD

We show estimates of the asymptotic variance of HSIC and MMD along a training trajectory in Figure 7. For MMD we consider both a single shuffling of the data (MMD-full), as well as a split shuffling (MMD-split) where we use half the data for our joint distribution sample, and the other half to permute for our product-of-marginals sample.

We note that the initial variance of MMD-split is substantially higher than that of MMD-full, which is much higher than the variance of HSIC. We hypothesize this makes the MMD-based objective harder to optimize, and gives a possible explanation for why MMD-split performs worse than MMD-full. MMD-split/full also exhibit greater final variances, particularly at larger batch sizes.

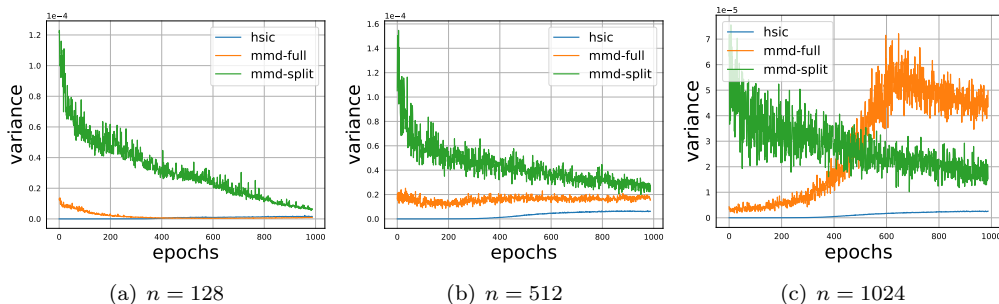


Figure 7: Estimates of the asymptotic variance of HSIC (blue), MMD with a single permutation (orange), and MMD with a split permutation (green) along a training trajectory for HDGM-10 at sample sizes  $n=128$  (a),  $n=512$  (b), and  $n=1024$  (c).

### B.5 Training Times

We compare the training times of all methods in Table 2. Our method is comparable in speed to C2ST and MMD, and vastly faster than the variational mutual information bound methods InfoNCE and NWJ since both those methods require function evaluations for *every* possible pair of samples at each training step.

Table 2: Approximate training times for the HDGM-30 problem over 1,000 epochs on a GeForce RTX 4060. Times are rounded to the nearest minute

	Training Time
HSIC	41 m
C2ST	34 m
MMD	44 m
InfoNCE	8 h 38 m
NWJ	8 h 42 m

## Appendix C. Experiment Details

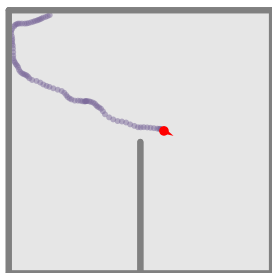


Figure 8: RatInABox simulation environment. The red dot is the current position of the rat and the purple circles indicate the past trajectory over 5 seconds. The box is designed to have only a single protruding wall.

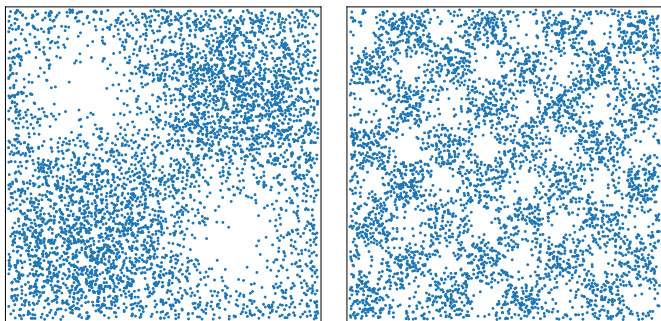


Figure 9: Samples drawn from the sinusoidal problem with frequency  $\ell = 1$  (left) and  $\ell = 4$  (right). We consider the latter frequency in our experiments.

### C.1 Training & Test Details

We design the featurizers  $\phi_\omega$  and  $\phi_\kappa$  of our deep kernels  $k_\omega$  and  $l_\kappa$  to be neural networks with ReLU activations. We avoid using normalization as it may affect test power. Moreover, we make the Gaussian bandwidth of both  $k_\omega$  and  $l_\kappa$  a learnable parameter, as well as the smoothing rate  $\epsilon$ . To make comparisons as fair as possible, we use similar neural network architectures for each deep learning based method. In general, we let the featurizer of HSIC-D and MMD-D be identical up to a concatenation layer which concatenates  $X$  and  $Y$  to frame the problem as a two-sample test. We construct the C2ST-S/L classifier as the MMD-D featurizer plus a linear layer classification head with scalar output, and we let both C2ST-S/L and InfoNCE use identical architectures for the classifier and critic. Detailed descriptions of each architecture are demonstrated in the following subsections.

All optimization-based methods (HSIC-D/Dx/O, MMD-D, C2ST-S/L, InfoNCE) are first trained on an identical split of the data, and then tested on the remaining split. In contrast, HSIC-M selects the median bandwidth based on the entire dataset, and is evaluated on the test set. We train our models using the AdamW optimizer with a learning rate of  $1e-4$  over 1,000 epochs for HDGM and RatInABox and 10,000 epochs for Sinusoid. We use a batch size of 512. All methods are implemented in PyTorch and trained on a NVIDIA A100SXM4 GPU.

Once learned, each methods' empirical power is evaluated on 100 test sets  $(S_Z^{te_1}, \dots, S_Z^{te_{100}})$ . Each test set contains  $m$  test samples  $S_Z^{te_i} = (Z_1^{te_i}, \dots, Z_N^{te_i})$ , which are then used to compute the average rejection rate under the null via a permutation test. We use 500 permutations for each test and with a predetermined type-I error rate of 0.05.

## C.2 Architectures

In all experiments we consider deep kernels with Gaussian feature and smoothing kernels  $\kappa$  and  $q$ , where each bandwidth is a trainable parameter randomly initialized around 1.0. We let the smoothing weight  $\epsilon$  also be a learnable parameter initialized to 0.01. No batch normalization is used and all hidden layers use ReLU activations. Dataset-specific designs are elaborated below.

**High-dimensional Gaussian mixture.** We use a feed-forward network for our deep kernel featurizer with latent dimensions  $2d, 3d$ , and  $2d$ . Details of each model is given in Table 3.

**Sinusoid.** The deep kernel featurizer is taken to be a feed-forward network with widths  $1 \times 8 \times 12 \times 8$ . C2st, infoNCE, and NWJ use a similar architecture –one with widths  $2 \times 8 \times 12 \times 8 \times 1$ – which includes an additional scalar output layer.

**RatInABox.** We use a feed-forward featurizer with details given in Table 4. Unlike the previous two problems, the sample spaces  $\mathcal{X}$  and  $\mathcal{Y}$  are not equivalent, and so the deep featurizers for  $k$  and  $l$  have different architectures.

dataset	model	input	featurizer
HDGM-4	HSIC-D	X or Y	[ 2 → 4 → 6 → 4 ]
	MMD-D	[X, Y]	[ 4 → 8 → 12 → 8 ]
	C2ST-S/L	[X, Y]	[ 4 → 8 → 12 → 8 → 1 ]
HDGM-8	HSIC-D	X or Y	[ 4 → 8 → 12 → 8 ]
	MMD-D	[X, Y]	[ 8 → 16 → 24 → 16 ]
	C2ST-S/L	[X, Y]	[ 8 → 16 → 24 → 16 → 1 ]
HDGM-10	HSIC-D	X or Y	[ 5 → 10 → 15 → 10 ]
	MMD-D	[X, Y]	[ 10 → 20 → 30 → 20 ]
	C2ST-S/L	[X, Y]	[ 10 → 20 → 30 → 20 → 1 ]
HDGM-20	HSIC-D	X or Y	[ 10 → 20 → 30 → 20 ]
	MMD-D	[X, Y]	[ 20 → 40 → 60 → 40 ]
	C2ST-S/L	[X, Y]	[ 20 → 40 → 60 → 40 → 1 ]

dataset	model	input	featurizer
HDGM-30	HSIC-D	X or Y	[ 15 → 30 → 45 → 30 ]
	MMD-D	[X, Y]	[ 30 → 60 → 90 → 60 ]
	C2ST-S/L	[X, Y]	[ 30 → 60 → 90 → 60 → 1 ]
HDGM-40	HSIC-D	X or Y	[ 20 → 40 → 60 → 40 ]
	MMD-D	[X, Y]	[ 40 → 80 → 120 → 80 ]
	C2ST-S/L	[X, Y]	[ 40 → 80 → 120 → 80 → 1 ]
HDGM-50	HSIC-D	X or Y	[ 25 → 50 → 75 → 50 ]
	MMD-D	[X, Y]	[ 50 → 100 → 150 → 100 ]
	C2ST-S/L	[X, Y]	[ 50 → 100 → 150 → 100 → 1 ]

Table 3: Featurizer architectures used in deep kernels for HSIC-D, MMD-D, and classifier architecture used for C2ST-S/L on the HDGM problem. Brackets denote a sequence of linear layers with corresponding input and output features.

method	input	network
HSIC-D	X	[ 8 → 32 → 64 → 32 ]
	Y	[ 2 → 4 → 8 → 4 ]
MMD-D	[X, Y]	[ 10 → 32 → 64 → 32 ]
C2ST-S/L	[X, Y]	[ 10 → 32 → 64 → 32 → 1 ]

Table 4: Featurizer architectures used in deep kernels for HSIC-D, MMD-D, and classifier architecture used for C2ST-S/L on the RatInABox problem. Brackets denote a sequence of linear layers with corresponding input and output features.